HOKKAIDO UNIVERSITY

Title	Enhancement Mechanism of Microbial Current Production by Conductive Iron Sulphides Biosynthesized by Sulphate Reducing Bacteria
Author(s)	Muralidharan, Murugan
Degree Grantor	北海道大学
Degree Name	博士(理学)
Dissertation Number	甲第14011号
Issue Date	2020-03-25
DOI	https://doi.org/10.14943/doctoral.k14011
Doc URL	https://hdl.handle.net/2115/80666
Type	doctoral thesis
File Information	Murugan_Muralidharan.pdf

Hokkaido University Collection of Scholarly and Academic Papers : HUSCAP

Enhancement Mechanism of Microbial Current Production by Conductive Iron Sulphides Biosynthesized by Sulphate Reducing Bacteria

（硫酸還元細菌により生合成された導電性硫化鉄による微生物生成電流増大機構に関する研究）

Muralidharan MURUGAN

Graduate School of Chemical Sciences and Engineering

Hokkaido University



2020

Acknowledgement

I would like to express my sincere gratitude for my advisor Associate Professor, Dr. Akihiro Okamoto for the continuous support and guidance to carry out research throughout my doctoral study. Knowledges that I receive under my supervisor helped me to design and perform various scientific experiments and groomed me towards being more professional. I would be grateful to him for believing on me and providing excellent research environments.

I would like to show my special regards to Dr. Hidenori Noguchi, for his kind support, valuable advices and guidance during my doctoral study. I am indebted to Dr. Kohei Uosaki for his advises, useful discussions and providing me an opportunity to join as a Ph.D. student at GREEN, National Institute for Materials Science (NIMS).

I wish to thank all of the doctoral committee members Dr. Dairi Tohru, Dr. Jinhua Ye, Dr. Kazuyasu Sakaguchi, Dr. Masuda Takuya for their valuable feedbacks, guidance and encouragements at various stages. I sincerely thank all of my group members for their support and discussions that helped me to learn a lot as a researcher.

I wish to show my sincerely acknowledgement to National Institute for Materials Science (NIMS) for providing me NIMS junior researcher fellowship and Hokkaido University for providing me opportunity to do my doctoral study. My heartful thanks to all the administrative staffs for their kind support and assistances.

My sincere thanks go to all of my friends who constantly supported me in various aspects.

Last but not the least, I express my acknowledgement to my parents for their constant love, support and sacrifices that is always fuelling me to achieve greater heights.

Muralidharan Murugan

Tsukuba

February 2020

Table of Contents

Chapter 1 Introduction…….....1

1.1 General Introduction…….....….....1

1.2 Need for Microbial Fuel Cells as a renewable fuel source …….....1

1.2.1 Working principle of Microbial Fuel Cells……..……1

1.3 Sediment Microbial Fuel Cell (SMFC) as a technology for uninterrupted power supply …….....3

1.3.1 Application of SMFCs …….....5

1.3.1.1 SMFCs as renewable power source…….....5

1.3.1.2 SMFC mediated organic matter and pollutants removal…….....6

1.3.2 Challenges in SMFC technologies …….....7

1.4 Electroactive bacterial communities in the Microbial fuel cells 8

1.5 Electrical interactions and electron transport mechanisms from the electroactive microorganisms and the electrode…….....8

1.5.1 Direct electron transfer via conductive pili 8

1.5.2 Direct electron transfer via redox-active proteins 9

1.5.3 In-direct electron transfer via electron shuttles 9

1.6 Sulphate reduction at the aquatic sediments 10

1.6.1 Iron sulphide mineralization by Sulphate reducing bacteria at marine sediments…….11

1.7 Impact of biomineralized iron sulphides on bacterial electricity generation….....12

1.8 Objectives and Outline of the Present Thesis…….12

Reference…….16

Chapter 2 Experimental….....27

2.1 Bacteria cultivation.....27

2.2 Electrochemical setup and operation.....27

2.3 Scanning electron microscopy and X-ray photoelectron spectroscopy analysis……28

2.4 Coculture electro chemical experiments.....28

2.5 Electrochemical gating experiments with interdigitated

microelectrode array 29
2.6 Bioagglomerates embedding for thin sections.....29
2.7 Fluorescence in situ hybridization 30
2.8 Bottled experiments for FeS precipitation and quantifying dry weight…….....30
2.9 Quantification of total protein content…….……..30
2.10 Quantification of total bacterial cell counts…….....31
2.11 Electrochemical experiments with different metal ions…….……..31
Reference……...32

Chapter 3 Biosynthesized Iron Sulphide Nano Clusters Enhanced Anodic Current Generation by the Sulphate Reducing Bacteria…….....33
3.1 Introduction…….....33
3.2 Results and discussion…….....34
3.2.1 Anodic current generation by *Desulfovibrio vulgaris* Hildenborough.....34
3.2.2 FeS mediates electron transport from metabolic lactate oxidation to the electrode…….……...38
3.2.3 The mechanical insight of FeS-mediated current production …….....41
3.2.4. Sulphide oxidation coupled anodic current generation……43
3.2.5. Comparison of SRB mediated anodic current with IRB……45
3.3 Conclusion…….....45
References….....46

Chapter 4 Iron sulphide nanoclusters induced synergetic relationship between Sulphate Reducing Bacteria and Iron Reducing Bacteria coculture systems.....51
4.1 Introduction.....51
4.2 Results and discussion.....52
4.2.1 Synergetic current generation in SRB and IRB co-cultures ……..……52
4.2.2 Iron sulphides production couples with the synergetic current production in the coculture.....54
4.2.3 Enhancement of conductive networks in the coculture system.....56
4.2.4 Need to investigate electron transfer across bioagglomerates ……...……58
4.2.5 Source-drain experiments to study the bioagglomerate

conductive properties.....58
4.2.6 FeS based long range electron transfer in the bioagglomerates.....59
4.3 Conclusion.....62
References.....63

Chapter 5 Iron reducing bacteria enhanced synergetic growth and iron sulphide bio precipitation in the sulphate reducing bacteria.....64
5.1 Introduction.....64
5.2 Results and discussion.....65
5.2.1 Iron reducing bacteria dependent iron sulphides bio precipitation.....65
5.2.2 Accelerated microbial activity inside the cocultures.....66
5.2.3 Increased microbial growth in SRB and IRB coculture system.....67
5.2.4 Synergetic growth between SRB and IRB cells 69
5.2.5 Proposal for accelerated FeS generation by SRB in the presence of IRB.....71
5.3 Conclusion.....71
References.....72

Chapter 6 Microbial current generation enhancement by metal sulphide with better conductive properties.....73
6.1 Introduction.....73
6.2 Results and Discussion.....74
6.2.1 Microbial electricity generation with different metal ions.....74
6.2.2 Microbial electricity generation with different metal ions in the presence of FeS bioprecipitates 75
6.3 Conclusion.....77
References.....78

Chapter 7 General conclusion and future prospects.....80
7.1 General Conclusion.....80
7.2 Future Prospects.....81

Chapter 1

Introduction

1.1 General introduction

The consumption and demand of energy around the globe is undeniably increasing and in terms of energy sources the non-renewable energy sources like fossil fuels and nuclear energy still accounts for an enormous share of energy consumed by the global countries.[1-2] The energy derived from the fossil fuels served as the backbone for the industrial revolution which however has its own grey side. Carbon dioxide emissions from burning fossil fuels is causing huge environmental and ecological problems in the 21st century.[3] Nuclear energy and nuclear power plants proved to be catastrophic in previous incidents because of the emission of nuclear radiations and unavailable long-term protocol to dispose nuclear wastes sustainably. [4]

1.2 Need for Microbial Fuel Cells as a renewable fuel source

The focus on using renewable energy sources are increasing exponentially in areas like solar, wind, tidal, hydro power and biomass energy generation.[5-10] In addition to them, the usage of bio electrochemical systems (BES) has recently gained attention among the academic researchers in recent decades. A BES, mimics the bacterial interaction with the insoluble electron donors and acceptors. Microbial Fuels Cell (MFC) is the most extensively studied BES where bacteria oxidize organic and inorganic matter and generate electricity.[11] The MFC works similar to that of a traditional fuel cell where the microorganisms which can use a range of organic fuel sources for converting the energy stored in the chemical bonds into electricity.[12-14]

1.2.1 Working principle of Microbial Fuel Cells

The original idea of using microbes for electricity generation was initiated in 1911 and then the practical developments with catalysts and synthetic mediators were made in the later periods.[14-17] Microorganisms like bacteria can produce electrical energy by oxidizing organics substrates and even biodegradable substrates from the waste water simultaneously applying for treatment opportunities for municipal waste waters.[12, 18] Electrons which are produced from the oxidation of

the substrates are transferred to the anode from the electroactive bacteria. Usually the anodic part of the MFCs are maintained anaerobic to facilitate the growth of anaerobic bacteria which are capable of donating electrons to the anodes such as *Geobacter sulfurreducens* which are obligatory anaerobic bacteria.[19] Also, maintaining an anaerobic condition eliminates the electron acceptor oxygen. The active microbial biocatalysts oxidize the organic substrates in to form electrons and protons. A typical oxidation reaction catalyzed by the anode grown electro active bacteria is shown below where acetate is oxidized at the anodic chamber.

$$CH_3COO^- + 4H_2O \rightarrow 2HCO_3^- + 9H^+ + 8e^- \quad (1)$$

The protons are transferred to the cathode chamber through a proton exchange membrane (PEM) and the electrons are conducted to the cathode by and external circuit.[3, 11] The migrated protons combine with electrons and a catholyte such as oxygen which gets reduced on the cathode surface. The oxygen is major oxidant on cathodes because of its abundance and high reduction potential. The oxygen reduction reaction (ORR) generates production of water which can be shown as below.

$$O_2 + 4H^+ + 4e^- \rightarrow 2H_2O \quad (2)$$

This reaction establishes the flow of electrical current similar to that of a chemical fuel cell, except that the microbes act as the biocatalysts to generate electron and protons. Generally, the catalysts, increase the reaction rate without gaining energy form the reactions they catalyse or they don't get changed. However, in case of electroactive microbes at MFC anodes, it's not the same as they utilize the energy obtained by oxidation for their growth and create energy loss. Hence, they as not true catalysts as they may gain all their carbon and energy requirements for cellular growth by the complex organic substrate oxidation and thus the MFC technology is self-sustainable. They can generate energy as long as the conditions for electro active microbes found on anode surface gets favourable energy source for their survival.[20-21]

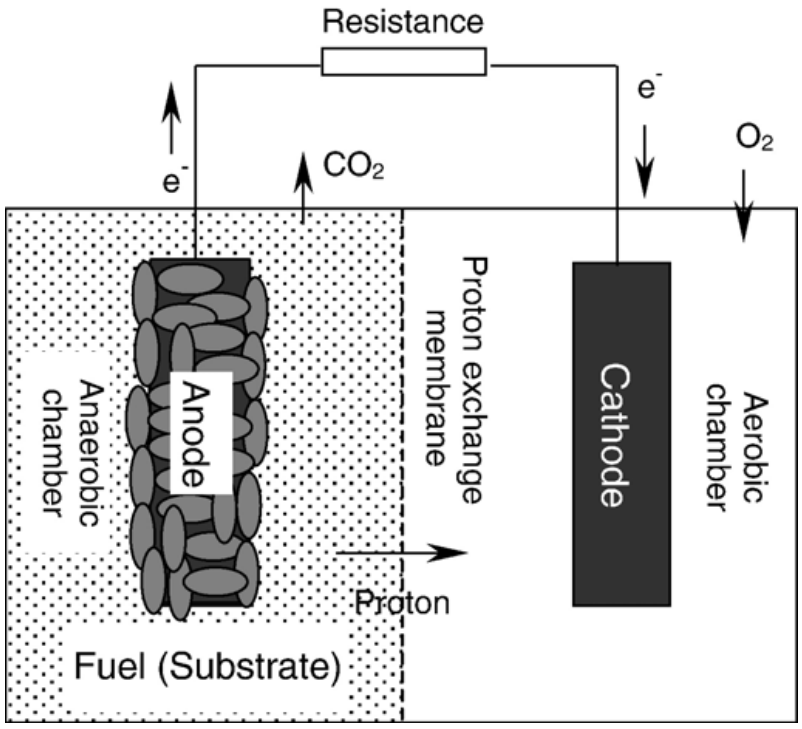


Figure 1-1 Schematic diagram of a typical two-chamber microbial fuel cell

1.3 Sediment Microbial Fuel Cell (SMFC) as a technology for uninterrupted power supply

At the anoxic subsurface environments and aquatic sediments, the organic matters that are formed by the degradation of dead organisms and plants has a large potential for energy source. One such form of energy is the petroleum which is a rich source of concentrated form of energy that is readily available for use. However, most of the other forms of organics are able to be used as energy source with current commercial technologies. These anoxic regions are usually inhabited by anaerobic subsurface microorganisms which rely on these organic sources for their survival. The MFC technologies can be applied at these environments to tap the energy stored at the subsurface environments. In SMFC, the electrical energy can be generated by placing an electrode into these anaerobic sediments which acts as anode which was connected to a similar electrode (cathode) in the overlying relatively aerobic marine water.[22-23] Thus, electroactive microorganisms form biofilms on the anode surface and donate electrons and protons. There is no need for separate PEM in this setup as the water filled pores in the sediments does the part of proton transfer to the overlying water. The current generated was sufficiently enough theoretically support low power

devices and when the sediment bacteria were killed, the electricity generation was affected.[23] Recently it has attracted many interests because of its capability to reduce organics in the sediments.[24]

The decomposition of organic matter in marine sediments utilizes a succession of oxidants based on energy of the reaction. In rich sediments, the oxygen reduction reaction can be found at the subsurface followed by nitrate, MnO_2, Fe_2O_3, and iron reduction within next few centimetres and the sulphate reduction can be observed after nearly one-meter depth. With increasing depth each layer is accumulated with potential reductants. These distinct chemical reactions happening at different depths develop a potential gradient across the marine sediments. This potential gradient can be utilized by placing electrodes that can resemble the fuel cell technology where the anode is kept buried inside the anoxic sediments connecting to a cathode electrode placed in the marine water. It is claimed that the electrons are derived to the anode by the direct action of electron transfer from the anode grown electrogenic microbes and also through dissolved and solid phase forms of reduced compounds formed in the sediments. For example, hydrogen sulphide produced by the action of Sulphate Reducing Bacteria (SRB) can get oxidized on the anodes. Unlike MFCs, a typical SMFC don`t require a PEM or redox mediators. The presence of uninterrupted flux of organic rich sediments ensure that the SMFC can operate SMFC indefinitely.[18, 23]

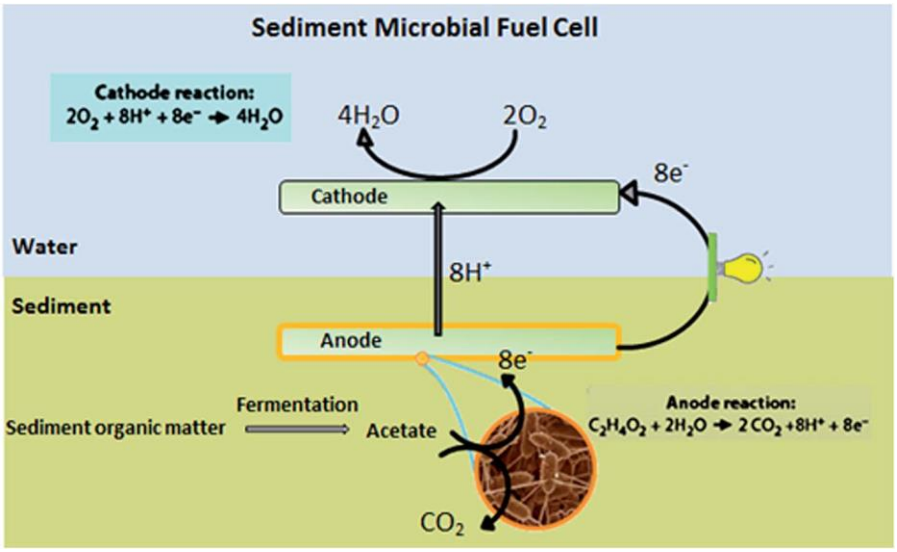


Figure 1-2 Schematic set up of a sediment microbial fuel cell.

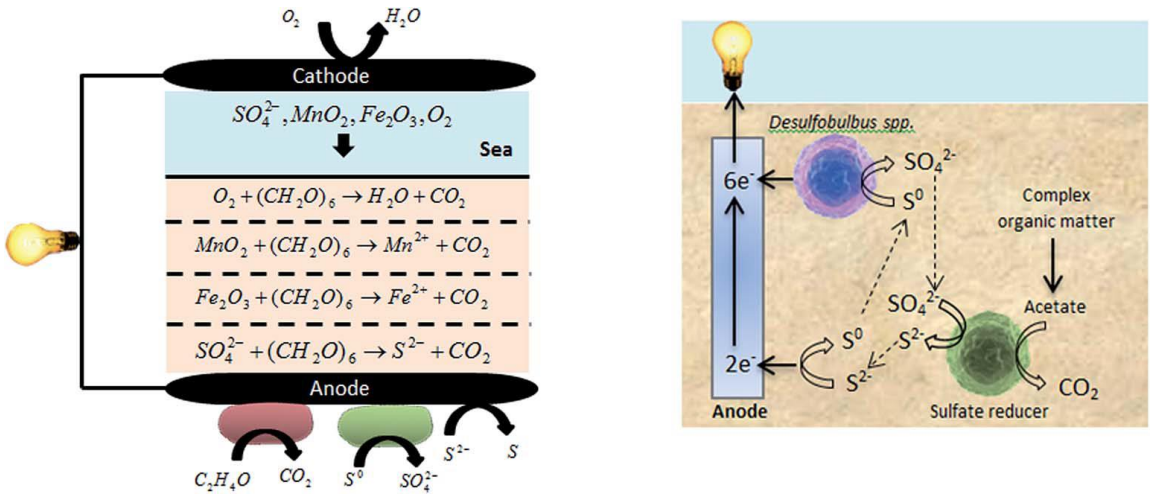


Figure 1-3 Microorganism roles and main reactions in SMFCs.

1.3.1 Application of SMFCs

The application of SMFCs can be broadly classified into two: (1) Acting as the energy source for electrical devices operating at marine environments, rivers, lakes, fresh waters and oceans for long term monitoring. (2) removal of unwanted organic wastes from the sediments.

1.3.1.1 SMFCs as renewable power source

Earlier studies have demonstrated that the SMFCs can be practically used to power meteorological buoy which measures air temperature, pressure, relative humidity and water temperature with a radio frequency communication system. Thus, they can readily power wireless devices used for environmental monitoring, oceanographic sensors and even military surveillance systems where real-time data acquisition from remote locations is required.[24-27] Usually these kind of instruments need a stable power supply. Since they cannot be connected with a wired power source, they need setup like batteries for power supply which however, is not effective in longer run and they need to be replaced periodically in the deep waters. This problem can be solved by using SMFCs as the power source. SMFCs has potential to be used for various wireless sensors that monitor temperature, salinity, tidal patterns, the presence of algae and other life forms, migration patterns of fish and other marine wildlife, organic contamination from oil production, metallic compounds from other industrial processes, pH, humidity, aquatic life, invasive species, and also biological oxygen demand (BOD) biosensors, and dissolved oxygen (DO) sensors.[24, 28-31]

1.3.1.2 SMFC mediated organic matter and pollutants removal

Organic-rich sediments which are an important component of aquatic environment can be considered as an abundant potential source of renewable energy. But the surface layer of the aquatic sediments is affected by the effluents of industrial wastewater and municipal sewage which are rich in pollutants such as organic matter, nitrogen, and phosphors, resulting in water-quality issues and even methane emission. These pollutants are lethal for marine organisms because of their carcinogenic and mutagenic properties. SMFCs has immense potential to remove these components by using them as fuel sources for their operation. The removal efficiency of the sedimental organic matters can be linearly related with the generated electricity.[32-34] Even, the microbial communities present at the anodes has the capability to reduce toxic heavy metals into their non-toxic forms. Thus, this opens the use of SMFCs as a tool for bioremediating toxic heavy metals. [35]

1.3.2 Challenges in SMFC technologies

Although demonstrations have been made with SMFCs as a power sources for instruments, a significant amount of SMFC research is still made on improving the SMFC performance with better electricity generation over a longer time frame. Areas to improve their performance is focussed on sedimental properties, overlying water, equipment configurations, operating conditions and electrode materials.

The microbes at the SMFC anodes are primarily depend on sedimental organic matters for their survival and hence their activity is dependent on the amount of organics present. The overall SMFC power output can be increased with higher sedimental organic matters. The usual proportion of sediment organic content ranges from 0.4% to 2.2% by weight.[3, 36] The sediments with higher flux of organics would be preferable for better power output.[37] The sedimental bed conductivity can be also impacting the performance of SMFCs. Sediments with more conductive materials can improve their conductivity therefore enabling electron conduction between microbes and anodes. Graphite flakes and colloidal iron hydroxides are studied as effective conductive materials for SMFC performance improvement.[38-39] Even the sediment pH can impact the power generation in SMFC.[40]

The parameters of sediment overlying water such as its nature, origin, flow conditions, characteristics, functional activities, total dissolved solids, pH and temperature can affect the function of the SMFCs. The power density of the SMFCs were found to be higher in case of stagnant water when compared to flowing water bodies. In addition, the dissolved oxygen content is a significant factor since oxygen is the electron acceptors at cathodes.

SMFC equipment configurations such as electrode spacing, water depth, depth of the embedded anode, the anode chamber, cathode arrangement is needed to be considered for a better performing system. AT different depths in sediments different microbial communities are found to be active which showed better anode performance at greater depths. Since each sedimental environments differ significantly, the anode embedding depths should be considered locally.

Similar to a typical MFC system, utilizing better electrode materials are always necessary for higher current densities. The electrode material, geometry and surface modifications are important factors in SMFC operations. These parameters are crucial for harvesting electricity from the sedimental microbes as they influence microbial adhesion to anode, electron transfer and substrate oxidation.[24, 41] Usually anodes should have better conductivity, environmental stability and better redox reversibility. Graphite, stainless steel and carbon materials are one of the most widely used anode materials. Several anode surface modification studies have been performed to increase its power density. SMFCs with low power densities require higher electrodes with higher surface area for powering the devices. This usually increases the cost of production of the SMFC devices. Hence it is crucial that the power densities of the electrodes are high enough to reduce the device costs.[42] At the cathodes, the electron transfer rate and oxygen reduction reaction are quite important phenomenon.[43] Even in some cases, the oxygen reduction reaction is catalysed by microorganisms growing on cathode surface, emerging the formation of bio-cathodes. It is usually cheap, has better sustainability and mediator less.[41, 44-45] Some of the common microbes at cathodes are oxygenic phototrophs and iron oxidizing bacteria. In some cases, even mixed bacterial cultures are found on the bio-cathodes.[45-46]

1.4 Electroactive bacterial communities in the Microbial fuel cells

A diverse range of microorganisms are found in association with electrodes in MFC systems, especially when an environmental inoculum is used to seed the MFC[22, 47-50]. A general

term for bacteria associated with a surface is a biofilm. It is likely that not all of the organisms associated anode biofilm interact directly with the anode but may interact indirectly through other members of the electrode community. For example, *Brevibacillus sp*. PTH1 was found to be an abundant member of a MFC community. Power production by *Brevibacillus sp. PTH1* is low unless it is cocultured with a *Pseudomonas sp*. Or supernatant from a MFC run with the *Pseudomonas sp*. Is added[51]. Pure cultures capable of producing current in a MFC include representatives of the Firmicutes and Acidobacteria, four of the five classes of Proteobacteria as well as the yeast strains *Saccharomyces cerevisiae* and *Hansenula anomala*[52-62]. These organisms interact with an anode through a variety of direct and indirect processes producing current to varying degrees.[20]

1.5 Electrical interactions and electron transport mechanisms from the electroactive microorganisms and the electrodes

Exoelectrogenic bacterial species have the ability to facilitate electron transfer via two mechanisms, direct and indirect electron transfer [63]. Direct electron transfer requires a physical connection between the bacterial cell and the electrode surface, namely nanowires and/or redox-active proteins. Indirect electron transfer does not require a physical connection but instead this mechanism relies on electron shuttling molecules[64]. There are currently three established methods of electron transfer (e.g. nanowires, membrane bound cytochromes and electron mediators) which bacteria can utilize to donate electrons to the anode in a MFC configuration [65].

1.5.1. Direct electron transfer via conductive pili

Bacterial colonies isolated in the anodic chamber of a fuel cell are incapable of transferring electrons directly to the electrode[12]. However, anodophiles have the ability to use electrons (in the anode) as their end electron acceptor. Thus, these specific bacterial species are involved in electron transfer, leading to the generation of an electrical charge. A major breakthrough in MFC technology was observed by Kim et al. who demonstrated that electron transfer does not always need mediator (electron transfer) compound molecules [66]. The bacterial cell surface of specific isolated bacterial species, such as *Shewanella spp*., and *Geobacter spp*., have utilize long proteinaceous filaments that extend from their outer surface into the extracellular matrix. These

appendages are thought to be involved in extracellular electron transport processes, referred to as microbial nanowires due to their long filament-like appearance and conductive attributes [67].

Nanowires can be either flagella or pili, both of which have very distinct properties, and therefore we propose the terms micro-nanowires and macro-nanowires. Traditionally, the major role of the flagellum of bacteria is to mediate the motility of the cell via swarming and swimming, allowing for colony expansion on a surface. One of the roles of Type IV pili is to mediate twitching to pull the cell across a surface (often in dense aggregates) [68]. Nanowires have the ability to partake in direct electron mediated transfer. Type IV pili play vital roles in secretion systems for effectors, microbial adherence and bacterial movement, establishing contact between the bacterial species and the electrode surface[69]. Reguera et al. showed that wild type *G. sulfurreducens* could attach to Fe (III) oxides after 48 h, as demonstrated by an increase in biomass. However, in the same time period, the pilA deficient strain could not grow, which was indicated by a decrease in biomass [70]. In regards to the bacterial species evaluated for electricity generation for potential application in microbial fuel cell technologies, *G. sulfurreducens* is currently the "gold standard", producing the highest recorded current densities of any known pure culture, utilizing micro-nanowires [71-73].

1.5.2. Direct electron transfer via redox-active proteins

Most studies suggest that the direct contact by pili of the conductive bacterial biofilms and the iron oxides is essential for the reduction of iron oxides. However, another mechanism of electron transfer requires redox active proteins and allows for short-range electron transfer to take place [74]. C-type cytochromes are commonly known for their primary function in mitochondria, as these molecules play a pivotal role in ATP synthesis[75]. Smith et al. revealed that deletion of the gene encoding for PilA, a structural pilin protein in the KN400 strain of *G. sulfurreducens* inhibited iron oxide reduction [76]. One possible explanation for the continued iron reduction even with structurally damaged pili is the utilization of c-type cytochromes, such as OmcS and OmcE [77].

1.5.3. In-direct electron transfer via electron shuttles

Bacteria can generate electricity due to the production of secondary metabolites, which are able to act as endogenous redox mediators, often referred to as electron shuttles. Electron shuttles are organic molecules with a low molecular weight that have the ability to catalyze both reduction and oxidation reactions, using for example phenazines and quinones [78]. Bacterial cells can utilize

both added/in solution (exogenous) or self-produced/on bacterial cell surface (endogenous) shuttle compounds for extracellular electron transfer. However, for effective electron transfer to take place, electron shuttles must be both chemically-stable and not easily biologically degraded [78]. Unlike conductive pili, electron shuttles eliminate the need of direct contact between the bacterial cell and the electron acceptor (which in the case of MFCs is the electrodes) [67]. Within the bacterial cells, electrons are first transported to the cell surface via a metabolic pathway, which involves redox-active proteins and low molecular weight compounds. Subsequently, electrons are then transported to cytochromes or potential shuttles in either the periplasm or the outermembrane [78]. Soluble electron shuttles can diffuse into the medium surrounding the bacterial cell, and once outside, the electrons can be transferred to suitable external acceptors, with examples including insoluble Fe (III) oxides or a MFC anode [78]. Some compounds shown to be effective electron shuttles include thionine, methyl viologen, 2- hydroxy-1,4-naphtoquinone, methylene blue, humic acids and anthraquinone- 2,6-disulfonic acid [79-82].

Other more common examples of electron shuttles are molecules known as flavins. Flavins demonstrate enhanced efficiency when partaking in biogeochemical iron cycles, and redox potentials, which improves electron transfer. Thus, flavins have the potential to be applied to MFC technologies as such molecules can be used as endogenous electron transfer mediators [83]. Further, the importance of flavins as electron shuttles, have been shown, as the concentration of flavins increased from 0.2 μm to 0.6 μm to 4.5–5.5 μm the peak current produced by S. oneidensis became four times greater [78]. Flavins are often produced as secondary metabolites in bacteria, for example, riboflavin which is also known as vitamin B_2. This compound has been shown to act as an electron shuttle by Marsili et al. when *S. oneidensis* biofilms were analysed [84]. Results showed that the removal of riboflavin from biofilms resulted in a reduction of electron transfer rate to the electrodes by more than 70% [84].

1.6 Sulphate reduction at the aquatic sediments

Throughout Earth's history the burial of solid phases of Fe and S has controlled the redox state of Earth's surface environments[85]. While iron is one of the most abundant elements on Earth, sulfur represents <1% of the Earth by mass [86], although its importance to life and earth systems is greater than its abundance would suggest. Though the sulfur cycle was the first elemental cycle to be studied, research on sulfur biogeochemistry is far from complete, and novel aspects of sulfur's

transformations on Earth are still being discovered[87]. In Earth's biosphere, sulfur may be gaseous (e.g., sulfur dioxide), dissolved (e.g., sulfide, polysulfides, thiosulfate, sulfite, or sulfate) or solid (e.g., metal sulfides, elemental sulfur). Much of the interest in sulfur is due to its redox versatility—from sulfide (−2) to sulfate (+6), with numerous redox transformations possible in between [88].

Microorganisms can take advantage of this diversity of oxidation states for energy conservation, which can be achieved by: (1) coupling the oxidation of organic compounds or dihydrogen to the reduction of oxidized organic and inorganic sulfur compounds (e.g., dimethyl sulfoxide, sulfate, elemental sulfur, and thiosulfate) [89-90]; (2) disproportionating elemental sulfur, thiosulfate and sulfite[91-92]; and (3) oxidizing organosulfur compounds, hydrogen sulfide, sulfur, sulfite, and thiosulfate chemosynthetically with oxygen and nitrate during respiration, or by anoxygenic photosynthesis[93].

Organic matter deposited on the seafloor provides food for the benthic communities, either at the sediment surface or upon burial into the sediment layers below. Oxygen is available for respiration and chemical reactions near the surface and through faunal burrows. Beneath this mixed surface zone, marine sediments constitute an anoxic world inhabited by anaerobic microorganisms. These subsurface organisms become increasingly sparse with depth, yet they account for half of all microbial cells in the ocean [94]. Their energy source in most of the seabed is the buried organic matter, which they oxidize to CO_2 and inorganic nutrients.

1.6.1 Iron sulphide mineralization by Sulphate reducing bacteria at marine sediments

Due to the high concentration of sulfate in seawater, sulfate generally penetrates meters down into the seabed and supplies the sulfate reducing bacteria (SRB) with an electron acceptor for their respiration. Sulfate is the dominant sulfur species at 28mM in the modern oxic oceans, while reduced sulfur species, including hydrogen sulfide and organosulfur compounds, are often abundant where oxygen is low or absent. In these low-oxygen environments, sulfur and iron can be immobilized in the form of iron sulfide minerals, primarily the iron(II) monosulfide mackinawite (tetragonal FeS), the iron(II,III) sulfide greigite (Fe_3S_4), and the iron (II) disulfide pyrite (FeS_2).[95-96]

Ninety-seven percent of the sulfide produced on Earth is attributable to the activity of sulfate-reducing bacteria (SRB) in low-temperature environments [93, 97] , while the remaining three

percent are produced at volcanoes and deep-sea hydrothermal vents [98-99]. SRB are present in an enormous diversity of environments including freshwater [100-101], hypersaline [102], hydrothermal sediment [103], polar [104-105], and oceanic crust [106] habitats.

1.7 Impact of biomineralized iron sulphides on bacterial electricity generation

The iron sulphides which are ubiquitous at the anoxic marine environments exhibit various biogeochemical processes by microbial interactions. Rather than an energy source for microbial interactions, these minerals exhibit various physical and conductivity properties which can be exploited by electrogenic microbes as well. They exhibit as microbially occurring electrical wires and shows electrocatalytic properties. Especially, mackinawite which exhibit metallic conductive properties can be utilized by electro active bacteria for performing extracellular electron transfer. In addition to iron sulphides, even iron oxides also showed better electrical conductive properties which helped intercellular and interspecies electron transfer mechanisms. They can electrically bridge discrete redox environments at the natural environments which can be observed at the marine sediments.

Even several reports showed that sedimentation of iron sulphides in microbial fuel cells and they are reported to be involved in electron transfers in microbial communities involved in bioremediation of industrial and mine waste water, biocorrosion and direct and indirect bioleaching. All forms of extracellular electron transport chain both direct and indirect ways might be involved in electron transfer to these metallic/ semi conductive minerals. Earlier reports showed better reports on extracellular electron transport chain mechanisms increased by Fe^{3+} and Mn^{4+} oxides.

In one earlier report, *Shewanella oneidensis* MR-1 used bioprecipitated iron sulphide minerals for increasing their EET current production. They used these minerals as conductors for long-distance electron transfer. The microbially generated electric current was seen to be one hundred folds larger than the current produced by Shewanella oneidensis MR-1 when there was no iron sulphide minerals. This extended the role of conductive iron sulphide minerals for enhancing the electron transfer efficiency of electro active microbes[108-111].

1.8 Objectives and Outline of the Present Thesis

The objective of this current thesis is to examine the role of biologically precipitated metal sulphides, especially the more conductive iron sulphide (FeS) nanoparticles on impacting the bacterial interactions and subsequently the microbial current generation at the anode surfaces. At the aquatic sediments, even though there might be competition between different microbes for survival with the limited organic sources, the SMFC anodes show growth of wide range microbial communities. This also rises questions on interaction among different bacterial species at the anodes. This work shows the involvement of SRB biomineralized iron sulphides and its impact on the current generation of pure SRB species and also with a coculture system with electro active bacteria. Utilization of limited organics by SRB for FeS biomineraliztion can affect the microbial current production by the Iron Reducing Bacteria (IRB) that are observed at the anode surface. We observed the synergetic microbial electrical generation, based on iron sulphide minerals and studied the conductive properties of the bioagglomerates formed on the anodes.

We used *Desulfovibrio vulgaris* Hildenborough and *Shewanella oneidensis* MR-1 as model species for SRB and IRB respectively. These two were the first to be performed with whole genome sequencing studies in their respective categories. Their metabolic pathways are well studied. They are used as the model organisms in various microbiological studies. Since both of these bacteria can efficiently utilize lactate as their electron donor for their energy production and the preculture growth culture mediums also contain lactate for their growth, we used lactate as the electron donors in their culture medium throughout the experiments.

In the SMFC systems, the anode which is usually buried inside the sediments is surrounded with microbial precipitates. Even though different studies have been conducted on the cathode improvements at SMFCs, the overall power density at the cathodes are almost one tenth lesser than that of anodic power densities even after trying with different materials such as graphite felts, disk, activated carbon and stainless steel. Moreover, much of the microbial interactions with electrodes happen at the anodes when compared to cathodes, which directly complies with our current objective. Hence, in the current study we focused on the microbial interaction at the andic surfaces by using an anodic half-cell bio-electrochemical system.

In Chapter 1, the general introduction for MFC, SMFC and their electricity generation mechanisms and designs are introduced. The mechanisms for direct and indirect extracellular electron mechanisms are briefly discussed followed by applications and challenges of SMFC systems. Biomineralization of conductive iron sulphides by sulphate reducing bacteria and past works based on microbial current enhancement by conductive nanoparticles are discussed.

In Chapter 2, the description of the experimental details such as the three-electrode electrochemical system design, microbial cultivation, conditions for electrochemical experiments, electrochemical measurements, characterization techniques like Scanning Electron Microscopy, Fluorescent In-Situ Hybridization and X-ray Photoelectron Spectroscopy Analysis are given.

In Chapter 3, the impact of FeS biosynthesis on the current production of SRB is explained. Desulfovibrio vulgaris Hildenborough has been used as a model organism to investigate the mechanism behind anodic current generation in SRB at sulfidic environments. The anodic current generation by SRB pure culture and the role of FeS on the current density is explained. The mechanism of FeS and hydrogen sulphide mediated anodic current generation is shown after analyzing the characterization results.

In Chapter 4, the current generation mechanism in SRB and IRB cocultures and its relation with the biomineralized FeS is discussed. *Shewanella oneidensis* MR-1 and *Desulfovibrio vulgaris* Hildenborough were used as the model organism for IRB and SRB respectively. Here, the dominance of FeS biomineralized by SRB on the coculture current is shown. The thickness of coculture bioagglomerates formed on the anode surface by making cross sectional thin sections and its electrical conductive properties by performing electrochemical gate experiments by interdigitated electrode array (IDA) are explained. Oxidation of FeS after lactate depletion and reduction in the conductive property of the coculture bioagglomerate is discussed.

In Chapter 5, the experimental data showing the symbiotic interaction of SRB and IRB are shown. Increase in the production of FeS bioprecipitates by SRB in the presence of IRB is discussed with experimental data measuring the increase in the dry weight of the system. The total protein concentration as a measurement of increase in the microbial growth is shown. The microscopic analysis showing increase in the IRB growth in the coculture system is explained.

This chapter deals with the symbiotic relationship between SRB and IRB for both growth and FeS generation.

In Chapter 6, the dependence of microbial electricity production by other metal sulphides are shown. Metal sulphides which have better electrical properties than FeS are made to bioprecipitate inside the coculture system. This chapter deals with methods to improve the MFC current density by using various metal sulphides with better electrical conductive properties and subsequently their potential for alternatively use the heavy metal sulphides for MFC performance improvement.

In Chapter 7, the general conclusion of the work and the future prospects are given.

Reference

1. Rahimnejad, M.; Ghoreyshi, A. A.; Najafpour, G.; Jafary, T., Power generation from organic substrate in batch and flow microbial fuel cell operations. *Applied Energy* **2011,** *88* (11), 3999-4004.

2. Akdeniz, F.; Çağlar, A.; Güllü, D., Recent energy investigations on fossil and alternative nonfossil resources in Turkey. *Energy Conversion and Management* **2002,** *43* (4), 575-589.

3. Rahimnejad, M.; Adhami, A.; Darvari, S.; Zirepour, A.; Oh, S.-E., Microbial fuel cell as new technology for bioelectricity generation: A review. *Alexandria Engineering Journal* **2015,** *54* (3), 745-756.

4. Schiermeier, Q.; Tollefson, J.; Scully, T.; Witze, A.; Morton, O., Energy alternatives: Electricity without carbon. *Nature* **2008,** *454* (7206), 816-823.

5. Slate, A. J.; Whitehead, K. A.; Brownson, D. A. C.; Banks, C. E., Microbial fuel cells: An overview of current technology. *Renewable and Sustainable Energy Reviews* **2019,** *101*, 60-81.

6. Granqvist, C. G., Transparent conductors as solar energy materials: A panoramic review. *Solar Energy Materials and Solar Cells* **2007,** *91* (17), 1529-1598.

7. Joselin Herbert, G. M.; Iniyan, S.; Sreevalsan, E.; Rajapandian, S., A review of wind energy technologies. *Renewable and Sustainable Energy Reviews* **2007,** *11* (6), 1117-1145.

8. Falcão, A. F. d. O., Wave energy utilization: A review of the technologies. *Renewable and Sustainable Energy Reviews* **2010,** *14* (3), 899-918.

9. Lund, J. W.; Freeston, D. H.; Boyd, T. L., Direct utilization of geothermal energy 2010 worldwide review. *Geothermics* **2011,** *40* (3), 159-180.

10. Rao, J. R.; Richter, G. J.; Von Sturm, F.; Weidlich, E., The performance of glucose electrodes and the characteristics of different biofuel cell constructions. *Bioelectrochemistry and Bioenergetics* **1976,** *3* (1), 139-150.

11. Logan, B. E.; Hamelers, B.; Rozendal, R.; Schröder, U.; Keller, J.; Freguia, S.; Aelterman, P.; Verstraete, W.; Rabaey, K., Microbial Fuel Cells: Methodology and Technology. *Environmental Science & Technology* **2006,** *40* (17), 5181-5192.

12. Du, Z.; Li, H.; Gu, T., A state of the art review on microbial fuel cells: A promising technology for wastewater treatment and bioenergy. *Biotechnol Adv* **2007,** *25* (5), 464-82.

13. Lovley, D. R., Microbial fuel cells: novel microbial physiologies and engineering approaches. *Current Opinion in Biotechnology* **2006,** *17* (3), 327-332.

14. Allen, R. M.; Bennetto, H. P., Microbial fuel-cells. *Applied Biochemistry and Biotechnology* **1993,** *39* (1), 27-40.

15. Karube, I.; Matsunaga, T.; Tsuru, S.; Suzuki, S., Continous hydrogen production by immobilized whole cells of Clostridium butyricum. *Biochimica et Biophysica Acta (BBA) - General Subjects* **1976,** *444* (2), 338-343.

16. Santoro, C.; Arbizzani, C.; Erable, B.; Ieropoulos, I., Microbial fuel cells: From fundamentals to applications. A review. *J Power Sources* **2017,** *356*, 225-244.

17. Potter, M. C., Electrical Effects accompanying the Decomposition of Organic Compounds. *Proceedings of the Royal Society of London. Series B, Containing Papers of a Biological Character* **1911,** *84* (571), 260-276.

18. Habermann, W.; Pommer, E. H., Biological fuel cells with sulphide storage capacity. *Applied Microbiology and Biotechnology* **1991,** *35* (1), 128-133.

19. Pant, D.; Van Bogaert, G.; Diels, L.; Vanbroekhoven, K., A review of the substrates used in microbial fuel cells (MFCs) for sustainable energy production. *Bioresource Technology* **2010,** *101* (6), 1533-1543.

20. Franks, A. E.; Nevin, K. P., Microbial Fuel Cells, A Current Review. *Energies* **2010,** *3* (5), 899-919.

21. Lovley, D. R., Bug juice: harvesting electricity with microorganisms. *Nature Reviews Microbiology* **2006,** *4* (7), 497-508.

22. Bond, D. R.; Holmes, D. E.; Tender, L. M.; Lovley, D. R., Electrode-Reducing Microorganisms That Harvest Energy from Marine Sediments. *Science* **2002,** *295* (5554), 483-485.

23. Reimers, C. E.; Tender, L. M.; Fertig, S.; Wang, W., Harvesting Energy from the Marine Sediment−Water Interface. *Environmental Science & Technology* **2001,** *35* (1), 192-195.

24. Zabihallahpoor, A.; Rahimnejad, M.; Talebnia, F., Sediment microbial fuel cells as a new source of renewable and sustainable energy: present status and future prospects. *RSC Advances* **2015,** *5* (114), 94171-94183.

25. Tender, L. M.; Gray, S. A.; Groveman, E.; Lowy, D. A.; Kauffman, P.; Melhado, J.; Tyce, R. C.; Flynn, D.; Petrecca, R.; Dobarro, J., The first demonstration of a microbial fuel cell as a

viable power supply: Powering a meteorological buoy. *Journal of Power Sources* **2008,** *179* (2), 571-575.

26. Sacco, N. J.; Figuerola, E. L. M.; Pataccini, G.; Bonetto, M. C.; Erijman, L.; Cortón, E., Performance of planar and cylindrical carbon electrodes at sedimentary microbial fuel cells. *Bioresource technology* **2012,** *126*, 328-335.

27. Donovan, C.; Dewan, A.; Heo, D.; Beyenal, H., Batteryless, Wireless Sensor Powered by a Sediment Microbial Fuel Cell. *Environmental Science & Technology* **2008,** *42* (22), 8591-8596.

28. Gong, Y.; Radachowsky, S. E.; Wolf, M.; Nielsen, M. E.; Girguis, P. R.; Reimers, C. E., Benthic Microbial Fuel Cell as Direct Power Source for an Acoustic Modem and Seawater Oxygen/Temperature Sensor System. *Environmental Science & Technology* **2011,** *45* (11), 5047-5053.

29. Scott, K.; Cotlarciuc, I.; Hall, D.; Lakeman, J. B.; Browning, D., Power from marine sediment fuel cells: the influence of anode material. *Journal of Applied Electrochemistry* **2008,** *38* (9), 1313.

30. Zhang, F.; Tian, L.; He, Z., Powering a wireless temperature sensor using sediment microbial fuel cells with vertical arrangement of electrodes. *Journal of Power Sources* **2011,** *196* (22), 9568-9573.

31. Majumder, D.; Maity, J. P.; Chen, C.-Y.; Chen, C.-C.; Yang, T.-C.; Chang, Y.-F.; Hsu, D.-W.; Chen, H.-R., Electricity generation with a sediment microbial fuel cell equipped with an air-cathode system using photobacterium. *International Journal of Hydrogen Energy* **2014,** *39* (36), 21215-21222.

32. Song, T.-S.; Jiang, H.-L., Effects of sediment pretreatment on the performance of sediment microbial fuel cells. *Bioresource technology* **2011,** *102* (22), 10465-10470.

33. Yan, Z.; Song, N.; Cai, H.; Tay, J.-H.; Jiang, H., Enhanced degradation of phenanthrene and pyrene in freshwater sediments by combined employment of sediment microbial fuel cell and amorphous ferric hydroxide. *Journal of Hazardous Materials* **2012,** *199-200*, 217-225.

34. Song, T.-S.; Yan, Z.-S.; Zhao, Z.-W.; Jiang, H.-L., Removal of organic matter in freshwater sediment by microbial fuel cells at various external resistances. *Journal of Chemical Technology & Biotechnology* **2010,** *85* (11), 1489-1493.

35. Abbas, S. Z.; Rafatullah, M.; Khan, M. A.; Siddiqui, M. R., Bioremediation and Electricity Generation by Using Open and Closed Sediment Microbial Fuel Cells. *Frontiers in Microbiology* **2019,** *9* (3348).

36. Byung Hong Kim, D. H. P., Pyung Kyun Shin, In Seop Chang, Hyung Joo Kim Mediator-less biofuel cell 5976719 1999.

37. Rezaei, F.; Richard, T. L.; Brennan, R. A.; Logan, B. E., Substrate-Enhanced Microbial Fuel Cells for Improved Remote Power Generation from Sediment-Based Systems. *Environmental Science & Technology* **2007,** *41* (11), 4053-4058.

38. Lenin Babu, M.; Venkata Mohan, S., Influence of graphite flake addition to sediment on electrogenesis in a sediment-type fuel cell. *Bioresource Technology* **2012,** *110*, 206-213.

39. Zhou, Y.-L.; Yang, Y.; Chen, M.; Zhao, Z.-W.; Jiang, H.-L., To improve the performance of sediment microbial fuel cell through amending colloidal iron oxyhydroxide into freshwater sediments. *Bioresource Technology* **2014,** *159*, 232-239.

40. Sajana, T. K.; Ghangrekar, M. M.; Mitra, A., Effect of operating parameters on the performance of sediment microbial fuel cell treating aquaculture water. *Aquacultural Engineering* **2014,** *61*, 17-26.

41. Wang, A.; Cheng, H.; Ren, N.; Cui, D.; Lin, N.; Wu, W., Sediment microbial fuel cell with floating biocathode for organic removal and energy recovery. *Frontiers of Environmental Science & Engineering* **2012,** *6* (4), 569-574.

42. Fu, Y.; Zhao, Z.; Liu, J.; Li, K.; Xu, Q.; Zhang, S., Sulfonated polyaniline/vanadate composite as anode material and its electrochemical property in microbial fuel cells on ocean floor. *Science China Chemistry* **2011,** *54* (5), 844-849.

43. Ren, Y.; Pan, D.; Li, X.; Fu, F.; Zhao, Y.; Wang, X., Effect of polyaniline-graphene nanosheets modified cathode on the performance of sediment microbial fuel cell. *Journal of Chemical Technology & Biotechnology* **2013,** *88* (10), 1946-1950.

44. Walter, X. A.; Greenman, J.; Ieropoulos, I. A., Oxygenic phototrophic biofilms for improved cathode performance in microbial fuel cells. *Algal Research* **2013,** *2* (3), 183-187.

45. Wetser, K.; Sudirjo, E.; Buisman, C. J. N.; Strik, D. P. B. T. B., Electricity generation by a plant microbial fuel cell with an integrated oxygen reducing biocathode. *Applied Energy* **2015,** *137*, 151-157.

46. Chen, Z.; Huang, Y.-c.; Liang, J.-h.; Zhao, F.; Zhu, Y.-g., A novel sediment microbial fuel cell with a biocathode in the rice rhizosphere. *Bioresource Technology* **2012,** *108*, 55-59.

47. Rabaey, K.; Boon, N.; Siciliano, S. D.; Verhaege, M.; Verstraete, W., Biofuel Cells Select for Microbial Consortia That Self-Mediate Electron Transfer. *Applied and Environmental Microbiology* **2004,** *70* (9), 5373.

48. Phung, N. T.; Lee, J.; Kang, K. H.; Chang, I. S.; Gadd, G. M.; Kim, B. H., Analysis of microbial diversity in oligotrophic microbial fuel cells using 16S rDNA sequences. *FEMS Microbiology Letters* **2004,** *233* (1), 77-82.

49. Aelterman, P.; Rabaey, K.; Pham, H. T.; Boon, N.; Verstraete, W., Continuous Electricity Generation at High Voltages and Currents Using Stacked Microbial Fuel Cells. *Environmental Science & Technology* **2006,** *40* (10), 3388-3394.

50. Kim, B. H.; Park, H. S.; Kim, H. J.; Kim, G. T.; Chang, I. S.; Lee, J.; Phung, N. T., Enrichment of microbial community generating electricity using a fuel-cell-type electrochemical cell. *Applied Microbiology and Biotechnology* **2004,** *63* (6), 672-681.

51. Pham, T. H.; Boon, N.; Aelterman, P.; Clauwaert, P.; De Schamphelaire, L.; Vanhaecke, L.; De Maeyer, K.; Höfte, M.; Verstraete, W.; Rabaey, K., Metabolites produced by Pseudomonas sp. enable a Gram-positive bacterium to achieve extracellular electron transfer. *Applied Microbiology and Biotechnology* **2008,** *77* (5), 1119-1129.

52. Park, H. S.; Kim, B. H.; Kim, H. S.; Kim, H. J.; Kim, G. T.; Kim, M.; Chang, I. S.; Park, Y. K.; Chang, H. I., A Novel Electrochemically Active and Fe(III)-reducing Bacterium Phylogenetically Related to Clostridium butyricum Isolated from a Microbial Fuel Cell. *Anaerobe* **2001,** *7* (6), 297-306.

53. Zhang, T.; Cui, C.; Chen, S.; Yang, H.; Shen, P., The direct electrocatalysis of Escherichia coli through electroactivated excretion in microbial fuel cell. *Electrochemistry Communications* **2008,** *10* (2), 293-297.

54. Zuo, Y.; Cheng, S.; Call, D.; Logan, B. E., Tubular Membrane Cathodes for Scalable Power Generation in Microbial Fuel Cells. *Environmental Science & Technology* **2007,** *41* (9), 3347-3353.

55. Zhao, F.; Rahunen, N.; Varcoe, J. R.; Chandra, A.; Avignone-Rossa, C.; Thumser, A. E.; Slade, R. C. T., Activated Carbon Cloth as Anode for Sulfate Removal in a Microbial Fuel Cell. *Environmental Science & Technology* **2008,** *42* (13), 4971-4976.

56. Borole, A. P.; O'Neill, H.; Tsouris, C.; Cesar, S., A microbial fuel cell operating at low pH using the acidophile Acidiphilium cryptum. *Biotechnology Letters* **2008,** *30* (8), 1367-1372.

57. Zhang, K.; Martiny, A. C.; Reppas, N. B.; Barry, K. W.; Malek, J.; Chisholm, S. W.; Church, G. M., Sequencing genomes from single cells by polymerase cloning. *Nature Biotechnology* **2006,** *24* (6), 680-686.

58. Bond, D. R.; Lovley, D. R., Evidence for Involvement of an Electron Shuttle in Electricity Generation by Geothrix fermentans</em&gt. *Applied and Environmental Microbiology* **2005,** *71* (4), 2186.

59. Holmes, D. E.; Nicoll, J. S.; Bond, D. R.; Lovley, D. R., Potential Role of a Novel Psychrotolerant Member of the Family Geobacteraceae, Geopsychrobacter electrodiphilus gen. nov., sp. nov., in Electricity Production by a Marine Sediment Fuel Cell. *Applied and Environmental Microbiology* **2004,** *70* (10), 6023.

60. Chaudhuri, S. K.; Lovley, D. R., Electricity generation by direct oxidation of glucose in mediatorless microbial fuel cells. *Nature Biotechnology* **2003,** *21* (10), 1229-1232.

61. Walker, A. L.; Walker, C. W., Biological fuel cell and an application as a reserve power source. *Journal of Power Sources* **2006,** *160* (1), 123-129.

62. Prasad, D.; Arun, S.; Murugesan, M.; Padmanaban, S.; Satyanarayanan, R. S.; Berchmans, S.; Yegnaraman, V., Direct electron transfer with yeast cells and construction of a mediatorless microbial fuel cell. *Biosensors and Bioelectronics* **2007,** *22* (11), 2604-2610.

63. Huang, L.; Regan, J. M.; Quan, X., Electron transfer mechanisms, new applications, and performance of biocathode microbial fuel cells. *Bioresource Technology* **2011,** *102* (1), 316-323.

64. Lovley, D. R., Electromicrobiology. *Annual Review of Microbiology* **2012,** *66* (1), 391-409.

65. Kumar, A.; Katuri, K.; Lens, P.; Leech, D., Does bioelectrochemical cell configuration and anode potential affect biofilm response? *Biochemical Society Transactions* **2012,** *40* (6), 1308-1314.

66. Kim, H. J.; Park, H. S.; Hyun, M. S.; Chang, I. S.; Kim, M.; Kim, B. H., A mediator-less microbial fuel cell using a metal reducing bacterium, Shewanella putrefaciens. *Enzyme and Microbial Technology* **2002,** *30* (2), 145-152.

67. Reguera, G.; McCarthy, K. D.; Mehta, T.; Nicoll, J. S.; Tuominen, M. T.; Lovley, D. R., Extracellular electron transfer via microbial nanowires. *Nature* **2005,** *435* (7045), 1098-1101.

68. Conrad, Jacinta C.; Gibiansky, Maxsim L.; Jin, F.; Gordon, Vernita D.; Motto, Dominick A.; Mathewson, Margie A.; Stopka, Wiktor G.; Zelasko, Daria C.; Shrout, Joshua D.; Wong, Gerard C. L., Flagella and Pili-Mediated Near-Surface Single-Cell Motility Mechanisms in P. aeruginosa. *Biophysical Journal* **2011,** *100* (7), 1608-1616.

69. Shi, W.; Sun, H., Type IV Pilus-Dependent Motility and Its Possible Role in Bacterial Pathogenesis. *Infection and Immunity* **2002,** *70* (1), 1.

70. Reguera, G.; Nevin, K. P.; Nicoll, J. S.; Covalla, S. F.; Woodard, T. L.; Lovley, D. R., Biofilm and Nanowire Production Leads to Increased Current in Geobacter sulfurreducens Fuel Cells. *Applied and Environmental Microbiology* **2006,** *72* (11), 7345.

71. Malvankar, N. S.; Tuominen, M. T.; Lovley, D. R., Biofilm conductivity is a decisive variable for high-current-density Geobacter sulfurreducens microbial fuel cells. *Energy & Environmental Science* **2012,** *5* (2), 5790-5797.

72. Badalamenti, J. P.; Krajmalnik-Brown, R.; Torres, C. I., Generation of High Current Densities by Pure Cultures of Anode-Respiring Geoalkalibacter spp. under Alkaline and Saline Conditions in Microbial Electrochemical Cells. *mBio* **2013,** *4* (3), e00144-13.

73. Tan, Y.; Adhikari, R. Y.; Malvankar, N. S.; Ward, J. E.; Nevin, K. P.; Woodard, T. L.; Smith, J. A.; Snoeyenbos-West, O. L.; Franks, A. E.; Tuominen, M. T.; Lovley, D. R., The Low Conductivity of Geobacter uraniireducens Pili Suggests a Diversity of Extracellular Electron Transfer Mechanisms in the Genus Geobacter. *Frontiers in Microbiology* **2016,** *7* (980).

74. Yue, H.; Khoshtariya, D.; Waldeck, D. H.; Grochol, J.; Hildebrandt, P.; Murgida, D. H., On the Electron Transfer Mechanism Between Cytochrome c and Metal Electrodes. Evidence for Dynamic Control at Short Distances. *The Journal of Physical Chemistry B* **2006,** *110* (40), 19906-19913.

75. Ow, Y.-L. P.; Green, D. R.; Hao, Z.; Mak, T. W., Cytochrome c: functions beyond respiration. *Nature Reviews Molecular Cell Biology* **2008,** *9* (7), 532-542.

76. Smith, J. A.; Tremblay, P.-L.; Shrestha, P. M.; Snoeyenbos-West, O. L.; Franks, A. E.; Nevin, K. P.; Lovley, D. R., Going Wireless: Fe(III) Oxide Reduction without Pili by <span

class="named-content genus-species" id="named-content-1">Geobacter sulfurreducens Strain JS-1. *Applied and Environmental Microbiology* **2014,** *80* (14), 4331.

77. Nevin, K. P.; Kim, B.-C.; Glaven, R. H.; Johnson, J. P.; Woodard, T. L.; Methé, B. A.; DiDonato, R. J., Jr.; Covalla, S. F.; Franks, A. E.; Liu, A.; Lovley, D. R., Anode Biofilm Transcriptomics Reveals Outer Surface Components Essential for High Density Current Production in Geobacter sulfurreducens Fuel Cells. *PLOS ONE* **2009,** *4* (5), e5628.

78. Velasquez-Orta, S. B.; Head, I. M.; Curtis, T. P.; Scott, K.; Lloyd, J. R.; von Canstein, H., The effect of flavin electron shuttles in microbial fuel cells current production. *Applied Microbiology and Biotechnology* **2010,** *85* (5), 1373-1381.

79. Bennetto, H. P.; Stirling, J. L.; Tanaka, K.; Vega, C. A., Anodic reactions in microbial fuel cells. *Biotechnology and Bioengineering* **1983,** *25* (2), 559-568.

80. Roller, S. D.; Bennetto, H. P.; Delaney, G. M.; Mason, J. R.; Stirling, J. L.; Thurston, C. F., Electron-transfer coupling in microbial fuel cells: 1. comparison of redox-mediator reduction rates and respiratory rates of bacteria. *Journal of Chemical Technology and Biotechnology. Biotechnology* **1984,** *34* (1), 3-12.

81. Newman, D. K.; Kolter, R., A role for excreted quinones in extracellular electron transfer. *Nature* **2000,** *405* (6782), 94-97.

82. Sund, C. J.; McMasters, S.; Crittenden, S. R.; Harrell, L. E.; Sumner, J. J., Effect of electron mediators on current generation and fermentation in a microbial fuel cell. *Applied Microbiology and Biotechnology* **2007,** *76* (3), 561-568.

83. Lee, Y.; Bae, S.; Moon, C.; Lee, W., Flavin mononucleotide mediated microbial fuel cell in the presence of Shewanella putrefaciens CN32 and iron-bearing mineral. *Biotechnology and Bioprocess Engineering* **2015,** *20* (5), 894-900.

84. Marsili, E.; Baron, D. B.; Shikhare, I. D.; Coursolle, D.; Gralnick, J. A.; Bond, D. R., Shewanella secretes flavins that mediate extracellular electron transfer. *Proceedings of the National Academy of Sciences* **2008,** *105* (10), 3968.

85. Berner, R. A., Sedimentary pyrite formation: An update. *Geochimica et Cosmochimica Acta* **1984,** *48* (4), 605-615.

86. Allègre, C. J.; Poirier, J.-P.; Humler, E.; Hofmann, A. W., The chemical composition of the Earth. *Earth and Planetary Science Letters* **1995,** *134* (3), 515-526.

87. Canfield, D. E.; Thamdrup, B.; Fleischer, S., Isotope fractionation and sulfur metabolism by pure and enrichment cultures of elemental sulfur-disproportionating bacteria. *Limnology and Oceanography* **1998,** *43* (2), 253-264.

88. Fossing, H., Distribution and fate of sulfur intermediates—sulfite, tetrathionate, thiosulfate, and elemental sulfur—in marine sediments. *Sulfur Biogeochemistry: Past and Present* **2004,** *379*, 97.

89. Widdel, F.; Bak, F., Gram-negative mesophilic sulfate-reducing bacteria. In *The prokaryotes*, Springer: 1992; pp 3352-3378.

90. Rabus, R.; Hansen, T. A.; Widdel, F., Dissimilatory sulfate-and sulfur-reducing prokaryotes. *The Prokaryotes: Prokaryotic Physiology and Biochemistry* **2013**, 309-404.

91. Bak, F.; Pfennig, N., Chemolithotrophic growth of Desulfovibrio sulfodismutans sp. nov. by disproportionation of inorganic sulfur compounds. *Archives of Microbiology* **1987,** *147* (2), 184-189.

92. Thamdrup, B.; Finster, K.; Hansen, J. W.; Bak, F., Bacterial disproportionation of elemental sulfur coupled to chemical reduction of iron or manganese. *Appl. Environ. Microbiol.* **1993,** *59* (1), 101-108.

93. Picard, A.; Gartman, A.; Girguis, P. R., What do we really know about the role of microorganisms in iron sulfide mineral formation? *Frontiers in Earth Science* **2016,** *4*, 68.

94. Kallmeyer, J.; Pockalny, R.; Adhikari, R. R.; Smith, D. C.; D'Hondt, S., Global distribution of microbial abundance and biomass in subseafloor sediment. *Proceedings of the National Academy of Sciences* **2012,** *109* (40), 16213-16216.

95. Schoonen, M. A., Mechanisms of sedimentary pyrite formation. *SPECIAL PAPERS-GEOLOGICAL SOCIETY OF AMERICA* **2004**, 117-134.

96. Rickard, D., Metastable Sedimentary Iron Sulfides. 2012; Vol. 65, pp 195-231.

97. Trudinger, P.; Chambers, L.; Smith, J., Low-temperature sulphate reduction: biological versus abiological. *Canadian Journal of Earth Sciences* **1985,** *22* (12), 1910-1918.

98. Elderfield, H.; Schultz, A., Mid-ocean ridge hydrothermal fluxes and the chemical composition of the ocean. *Annual Review of Earth and Planetary Sciences* **1996,** *24* (1), 191-224.

99. Andres, R.; Kasgnoc, A., A time-averaged inventory of subaerial volcanic sulfur emissions. *Journal of Geophysical Research: Atmospheres* **1998,** *103* (D19), 25251-25261.

100. Ramamoorthy, S.; Piotrowski, J. S.; Langner, H. W.; Holben, W. E.; Morra, M. J.; Rosenzweig, R. F., Ecology of sulfate-reducing bacteria in an iron-dominated, mining-impacted freshwater sediment. *Journal of environmental quality* **2009,** *38* (2), 675-684.

101. Sass, H.; Ramamoorthy, S.; Yarwood, C.; Langner, H.; Schumann, P.; Kroppenstedt, R.; Spring, S.; Rosenzweig, R., Desulfovibrio idahonensis sp. nov., sulfate-reducing bacteria isolated from a metal (loid)-contaminated freshwater sediment. *International journal of systematic and evolutionary microbiology* **2009,** *59* (9), 2208-2214.

102. Foti, M.; Sorokin, D. Y.; Lomans, B.; Mussman, M.; Zacharova, E. E.; Pimenov, N. V.; Kuenen, J. G.; Muyzer, G., Diversity, activity, and abundance of sulfate-reducing bacteria in saline and hypersaline soda lakes. *Appl. Environ. Microbiol.* **2007,** *73* (7), 2093-2100.

103. Jørgensen, B. B.; Isaksen, M. F.; Jannasch, H. W., Bacterial sulfate reduction above 100 C in deep-sea hydrothermal vent sediments. *Science* **1992,** *258* (5089), 1756-1757.

104. Ravenschlag, K.; Sahm, K.; Knoblauch, C.; Jørgensen, B. B.; Amann, R., Community structure, cellular rRNA content, and activity of sulfate-reducing bacteria in marine Arctic sediments. *Appl. Environ. Microbiol.* **2000,** *66* (8), 3592-3602.

105. Karr, E. A.; Ng, J. M.; Belchik, S. M.; Sattley, W. M.; Madigan, M. T.; Achenbach, L. A., Biodiversity of methanogenic and other Archaea in the permanently frozen Lake Fryxell, Antarctica. *Appl. Environ. Microbiol.* **2006,** *72* (2), 1663-1666.

106. Robador, A.; Jungbluth, S. P.; LaRowe, D. E.; Bowers, R. M.; Rappé, M. S.; Amend, J. P.; Cowen, J. P., Activity and phylogenetic diversity of sulfate-reducing microorganisms in low-temperature subsurface fluids within the upper oceanic crust. *Frontiers in microbiology* **2015,** *5*, 748.

107. Kondo, K.; Okamoto, A.; Hashimoto, K.; Nakamura, R., Sulfur-Mediated Electron Shuttling Sustains Microbial Long-Distance Extracellular Electron Transfer with the Aid of Metallic Iron Sulfides. *Langmuir* **2015,** *31* (26), 7427-34.

108. Vita, N.; Valette, O.; Brasseur, G.; Lignon, S.; Denis, Y.; Ansaldi, M.; Dolla, A.; Pieulle, L., The primary pathway for lactate oxidation in Desulfovibrio vulgaris. Frontiers in Microbiology 2015, 6 (606).

109. Heidelberg, J. F.; Seshadri, R.; Haveman, S. A.; Hemme, C. L.; Paulsen, I. T.; Kolonay, J. F.; Eisen, J. A.; Ward, N.; Methe, B.; Brinkac, L. M., The genome sequence of the anaerobic,

sulfate-reducing bacterium Desulfovibrio vulgaris Hildenborough. Nature biotechnology 2004, 22 (5), 554-559.

110. Pinchuk, G. E.; Geydebrekht, O. V.; Hill, E. A.; Reed, J. L.; Konopka, A. E.; Beliaev, A. S.; Fredrickson, J. K., Pyruvate and lactate metabolism by Shewanella oneidensis MR-1 under fermentation, oxygen limitation, and fumarate respiration conditions. Appl. Environ. Microbiol. 2011, 77 (23), 8234-8240.

111. Heidelberg, J. F.; Paulsen, I. T.; Nelson, K. E.; Gaidos, E. J.; Nelson, W. C.; Read, T. D.; Eisen, J. A.; Seshadri, R.; Ward, N.; Methe, B., Genome sequence of the dissimilatory metal ion–reducing bacterium Shewanella oneidensis. Nature biotechnology 2002, 20 (11), 1118-1123.

Chapter 2

Experimental

2.1. Bacteria cultivation

D. vulgaris Hildenborough was grown anaerobically in routine for 3 days at 30 ºC in Widdel and Pfennig (WP) medium, pH 7.0, containing Solution A (per 980 ml): 1.0 g $CaSO_4$, 1.0 g NH_4Cl, 0.5 g KH_2PO_4, 2.0 g $MgSO_4 \cdot 7H_2O$, 1.0 g yeast extract, 1 ml 0.1 % resazurin (redox indicator), and 20 mM lactate (as electron donor), Solution B (per 10 ml): 0.5 g $FeSO_4 \cdot 7H2O$, and solution C (per 10 ml); 0.1 g Ascorbic acid. Solution A was nitrogen purged and autoclaved, whereas solution B and C were syringe filtered. Solution A, B, and C were mixed in the ratio of 9.8: 0.1: 0.1 and nitrogen purged for more than 20 minutes. 0.05 ml of freezer stock of *D. vulgaris* Hildenborough was added in 20 ml of WP medium and placed in the incubator. In this medium, the metabolism of *D. vulgaris* Hildenborough leads to the production of H_2S, which reacts with Fe to form the black-colored FeS. The extent of cell growth was monitored by color change of the medium. The mutant strain of *D. vulgaris* Hildenborough (Δ*cycA*) lacking periplasmic type I tetraheme cytochrome (TpI-c3) which was constructed in previous work[108], and grew in the WP medium was also used for electrochemical experiments. *Shewanella oneidensis* MR-1 was grown aerobically in 15 ml of Luria−Bertani medium with shaking at 160 rpm for 24 h at 30°C. After that, the bacterial culture was centrifuged at 6000 rpm for 10 minutes and the resultant pellet was suspended in Defined Medium supplemented with 20mM lactate which was incubated to 12 h at 30°C.

2.2. Electrochemical setup and operation

Single chamber electrochemical cells with three electrodes configuration were used as previously described [109-110]. A tin-doped In_2O_3 (ITO) glass (average sheet resistance of 5.9 Ω/square, having surface area: 3.1 cm^2) was placed at the bottom of the reactor and used as the working electrode. Ag/AgCl (sat. KCl) and a platinum wire (approximate diameter of 0.1 mm) were used as the reference and counter electrodes, respectively. WP medium containing 20 mM sodium lactate (4.5 mL) without yeast was injected into an electrochemical cell as an electrolyte and the solution was purged with N_2 gas for more than 15 min to remove the dissolved O_2. Afterwards, 0.5 mL of a *D. vulgaris* Hildenborough grown cell suspension was injected into the

electrochemical cell. The electrochemical cell was connected to a potentiostat (VMP 3, Bio Logic Company) for electrochemical measurements. The electrochemical cell was maintained at 30 ºC throughout the experiment and the working electrode was poised at +0.2 V (vs Ag/AgCl [sat. KCl]) reference electrode. Linear sweep voltammograms (LSV) were measured at a scan rate of 1 mV s^{-1} with potential range of -0.5 to 0.5 V.

2.3. Scanning electron microscopy and X-ray photoelectron spectroscopy analysis

Sample preparation for SEM was performed by following the method previously reported [109]. On completion of electrochemical experiment, ITO electrode samples with attached microbes were carefully taken out from reactors and washed with 0.1 M phosphate buffer saline (PBS). Samples were fixed with 2.5 % glutaraldehyde prepared in 0.1 M PBS (pH 7.0) for 15 min. Afterwards, dehydration was carried out with an increasing ethanol series (25–50–75–100%, 10 min each). The samples were then dehydrated in t-butanol for 15 min, dried overnight under vacuum, coated with evaporated platinum and viewed using a JSM-7800F Scanning electron microscope (SEM) with Energy-dispersive X-ray spectroscopy (EDX). For X-Ray photoelectron spectroscopy, samples were vacuum dried and analyzed using X-Ray photoelectron spectroscope (AXIS Nova, Kratos) to study the surface composition of electrode biofilm.

2.4 Coculture electro chemical experiments

Single chamber three electrode electrochemical setup which was previously defined was used to check the anodic current generation studies. Tin doped In_2O_3 (ITO) glass (surface area: 3.1 cm^2, having average sheet resistance of 5.9 Ω/square) was the working electrode which was placed at the bottom of the EC reactor. A platinum wire with approximate diameter of 0.1 mm and Ag/AgCl (KCl Sat.) were used as counter and reference electrodes respectively. A modified WP medium with 25 mM HEPES and without yeast (4.75 ml) was used as the electrochemical reactor medium which has to be purged with O_2 free gas, for more than 15 min to remove dissolved oxygen, after injecting it to the EC reactor. Later the EC reactor was connected to the potentiostat (VMP 3, Bio Logic Company) for electrochemical measurements and maintained at a constant temperature of 30°C whereas the working electrode was poised at +0.2 (vs Ag/AgCl [sat. KCl]) reference electrode. 0.05 ml of washed *D.vulgaris* Hildenborough cell suspension grow after 3 days and 0.1 ml of washed and diluted *Shewanella oneidensis* MR-1 in DM medium was added to maintain a final OD_{600nm} of 10^{-4}. *D.vulgaris* Hildenborough was washed by centrifuging at 10000 rpm for 10

min and resuspending with the electrochemical reactor medium and the *Shewanella oneidensis* MR-1 was centrifuged at 6000 rpm for 10 mins and resuspended in fresh DM medium followed by dilution. Linear sweep voltammograms (LSV) were measured at a potential range of -0.5 to 0.5 V at 1 mV s^{-1}.

2.5 Electrochemical gating experiments with interdigitated microelectrode array

The source-drain experiments which were performed to identify long range electron conduction across the bioagglomerates employed interdigitated microelectrode array (IDA) as the working electrodes, as shown in previous studies[111]. IDAs consist of 10 µm wide parallel ITO micro electrode bands which were patterned onto a glass slide each separated 15 µm apart. The micro electrode bands are connected with opposite edge of the array leading to alternate interdigitated electrodes as electrode 1(E1) and electrode 2 (E2). This IDA was connected to a bipotentiostat for performing electrochemical measurements.

The bioagglomerates were grown by initially poising both E1 and E2 at +0.2 V vs Ag/AgCl (KCl Sat.) at 30°C until peak anodic current was observed where the bioagglomerates were thick enough to adjoin adjacent working electrode bands. For source-drain experiments, LSV was performed without and with a constant offset of +0.05 V between the E1 and E2 to perform them as electron source and electron drain across the bioagglomerates.

2.6 Bioagglomerates embedding for thin sections

The bioagglomerates formed on the ITO electrodes were embedded with technovit 8100 resin following the manufacturers protocol where ethanol was preferred for dehydration and sucrose infiltration step was omitted [112]. Initially the bioagglomerates were embedded with 1% (W/V) molten agar and allowed to solidify which was soon followed by fixation with 2% paraformaldehyde buffered with PBS for 1 h. This was then subjected to dehydration with increasing ethanol series (25–50–75–100%) with 10 min each placed on a rocker. Then the sample blocks were cut using Lecia microtome with a glass knife. The thin sections were cut with 1 µm thickness and stretched on a water droplet on a polylysine coated glass slide. The slides are then air dried and stored at room temperature until further analysis.

2.7 Fluorescence in situ hybridization

Fluorescence in situ hybridization (FISH) was performed to visualize the SRB and IRB distribution within the bioagglomerates. The hybridization was conducted with standard protocols[112], with SRB385 (5'-CGGCGTCGCTGCGTCAGG-3') and SHEW227 (5'-AGCTAATCCCACCTAGGTTCATC-3') as the probes for identifying SRB and IRB respectively, each marked with different fluorescent dyes. The hybridization was done with SRB385 and SHEW227 probes mixed with 40% formamide hybridization buffer. After hybridization, the cover slips were removed and gently washed with distilled water, followed by air drying. The hybridized samples were then visualized under a Lecia microscope with FITC and Texas red filters to visualize IRB and SRB respectively. DAPI stained thin sections were observed under microscope to identify the bioagglomerates cross sectional thin sections.

2.8 Bottled experiments for FeS precipitation and quantifying dry weight

A modified WP medium with 25 mM HEPES and without yeast (19.4 ml) was used as medium for bacterial growth which has to be purged with O_2 free gas, for more than 15 min to remove dissolved oxygen, after injecting it to a 25 ml glass bottles. To the glass bottles 0.2ml of three days cultivated *D.vulgaris* Hildenborough was added. Prior to addition the *D.vulgaris* Hildenborough was washed by centrifuging at 10000 rpm for 10 min. Then 0.4 ml of washed and diluted *Shewanella oneidensis* MR-1 in DM medium was added to maintain a final OD_{600nm} of $10^{-4.}$ The bottles are incubated at 30° C and the FeS precipitation was observed. The bioagglomerates precipitated inside the bottled cultures were isolated by centrifuging at 10000 rpm for 10 mins and then discarding the supernatant. The total wet weight was measured by subtracting the empty weight of the centrifuge tube with the centrifuge tube with bioagglomerates. Similarly the dry weight of the agglomerates were calculated after drying the tubes after centrifugation in an hot air over maintained at 60°C for 12 hours.

2.9 Quantification of total protein content

Initially the culture samples were centrifuged at 10000rpm for 10 mins to discard the supernatant to eliminate potent inhibitory substrates like ascorbic acid. Then the cells are re-dispersed in PBS solution and set for homogenization to disturb the bacterial cell wall. This can be performed by boiling the samples at 100°C for 10 minutes by adding 10% SDS. Then the

samples are taken for total protein content analysis by using a BCA protein analysis kit by following the manufacture`s protocol. The samples were mixed with working reagent with 1:20 ratio and incubated for 30 min at 37°C. After incubation the samples are taken to room temperatures and the absorbance was measured at 562 nm using a spectrophotometer.

2.10 Quantification of total bacterial cell counts

The bacterial cell counts were counted using a haemocytometer with a cover glass. The bacterial cell counts were counted within 1 mm^2 of area in the haemocytometer and the final bacterial cell counts in 1ml can be calculated by multiplying it with $10^{4.}$

2.11 Electrochemical experiments with different metal ions

Single chamber three electrode electrochemical setup which was previously defined was used to check the anodic current generation studies. Tin doped In_2O_3 (ITO) glass (surface area: 3.1 cm^2, having average sheet resistance of 5.9 Ω/square) was the working electrode which was placed at the bottom of the EC reactor. A platinum wire with approximate diameter of 0.1 mm and Ag/AgCl (KCl Sat.) were used as counter and reference electrodes respectively. 1.8mM of Fe^{2+} was added depending on the experimental requirements. A modified WP medium with 25 mM HEPES and without yeast (4.75 ml) was used as the electrochemical reactor medium which has to be purged with O_2 free gas, for more than 15 min to remove dissolved oxygen, after injecting it to the EC reactor. Later the EC reactor was connected to the potentiostat (VMP 3, Bio Logic Company) for electrochemical measurements and maintained at a constant temperature of 30°C whereas the working electrode was poised at +0.2 (vs Ag/AgCl [sat. KCl]) reference electrode. 0.05 ml of washed *D.vulgaris* Hildenborough cell suspension grow after 3 days and 0.1 ml of washed and diluted *Shewanella oneidensis* MR-1 in DM medium was added to maintain a final OD_{600nm} of 10^{-4}. *D.vulgaris* Hildenborough was washed by centrifuging at 10000 rpm for 10 min and resuspending with the electrochemical reactor medium and the *Shewanella oneidensis* MR-1 was centrifuged at 6000 rpm for 10 mins and resuspended in fresh DM medium followed by dilution. Addition of metal ions such as Cu^{2+}, Molybdate, Ni^{2+} and Mn^{2+} was performed during active FeS generation inside the reactor.

Reference

1. Sim, M. S.; Wang, D. T.; Zane, G. M.; Wall, J. D.; Bosak, T.; Ono, S., Fractionation of sulfur isotopes by Desulfovibrio vulgaris mutants lacking hydrogenases or type I tetraheme cytochrome c 3. *Front Microbiol* **2013,** *4*, 171.
2. Kondo, K.; Okamoto, A.; Hashimoto, K.; Nakamura, R., Sulfur-mediated electron shuttling sustains microbial long-distance extracellular electron transfer with the aid of metallic iron sulfides. *Langmuir* **2015,** *31* (26), 7427-7434.
3. Saito, J.; Hashimoto, K.; Okamoto, A., Flavin as an indicator of the rate-limiting factor for microbial current production in Shewanella oneidensis MR-1. *Electrochimica Acta* **2016,** *216*, 261-265.
4. Snider, R. M.; Strycharz-Glaven, S. M.; Tsoi, S. D.; Erickson, J. S.; Tender, L. M., Long-range electron transport in Geobacter sulfurreducens biofilms is redox gradient-driven. *Proc Natl Acad Sci U S A* **2012,** *109* (38), 15467-72.
5. McGlynn, S. E.; Chadwick, G. L.; Kempes, C. P.; Orphan, V. J., Single cell activity reveals direct electron transfer in methanotrophic consortia. *Nature* **2015,** *526* (7574), 531-5.

Chapter 3

Biosynthesized Iron Sulphide Nano Clusters Enhanced Anodic Current Generation by the Sulphate Reducing Bacteria

3.1 Introduction

Dissimilatory sulfate reducing bacteria (SRB) species take a major part of the microbial population in microbial fuel cells (MFCs). [1,2] Many studies showed that the electroactive sulfides derived from SRB were oxidized to elementary sulfur at the anode surfaces along with simultaneous bioelectricity generation, highlighting the valuable use of SRB for current generation along with sulfate removal in MFCs. [3–9] Abiotic oxidation of metabolically generated sulfide from sulfate by SRB has been proposed as the main mechanism of current production in MFCs. However, data in earlier reports have inferred that SRB is capable of directly transferring electrons to the extracellular electrodes. For example, earlier reports have shown growth of different SRB species over anode surfaces of the MFCs.[10] Also, electrode potential alteration caused significant gene upregulation in some SRB strains in metatranscriptomic analysis. However, most of the works on SRB with MFCs were related with sulfate removal studies and lack the in-depth knowledge on electron transfer mechanism from SRB to anode. Although electron uptake mechanisms by SRB have been widely investigated,[11,12] little is known about electron transfer in the reverse way i.e., direct electron transfer from SRB to insoluble electron acceptors, though understanding the mechanism of electron transfer by SRB to the anodes may give a better edge in extending the role of SRB for MFC current generation and further expanding its applications.

Beside current production mechanism via the oxidation of sulphide generated by SRB, the abundant availability of iron sulphides in the SRB sites might as well facilitate electron transfer to extracellular solids. The dissimilatory SRB, which naturally occur at anoxic subsurface regions such as marine sediments, are usually associated with biomineralization of iron sulphides such as pyrite, mackinawite, greigite and marcasite which have diverse electrical and electrocatalytic properties [13–19]. These iron sulphides have been also shown to be involved as naturally occurring electrical wires [18,20–24]. Electrically conductive nano particles have also been proposed to transport electron across outer membrane (OM) of Gram-Negative bacteria. Metal nanoparticles artificially synthesized on the cell surface enabled electron transfer from the cell interior across the OM to the

cell exterior, thereby functioning electron conductor across OM [25]. Similarly, it was proposed that the biosynthesis of FeS nano clusters attached on the cell surface might function as electron pathway across the OM for transfer of electrons to extracellular anodes in the presence of biomineralized iron sulphides [21,26]. Given direct electron transport mechanism has faster kinetics compared with diffusive electron shuttle[27], potential direct electron transport mechanism through iron sulphides may be more efficient compared with the current production via the anode oxidation of diffusing species of sulphide.

In the present study, we examined the impact of FeS biosynthesis on the current production of SRB using *Desulfovibrio vulgaris* Hildenborough, which has been used as a model organism to investigate the mechanism behind anodic current generation in SRB at sulphidic environments [28,29]. We conducted whole-cell electrochemical assays with *D. Vulgaris* Hildenborough in the presence and absence of biosynthesized FeS under anodic condition in three-electrode system. We also characterize the oxidation state of FeS produced on the surface of electrode during current production by X-ray Photoelectron Spectroscopy (XPS).

3.2 Results and discussion

3.2.1. Anodic current generation by *Desulfovibrio vulgaris* Hildenborough

To examine anodic current generation by the SRB in the presence of FeS, *D. vulgaris* Hildenborough was added to an Electrochemical (EC) system with the electrolyte for EC system contained WP medium supplemented with 20 mM lactate, 17 mM sulphate and 1.8 mM Fe^{2+}. As shown in Trace 1 of Figure 3-1, a steep increase in anodic current was observed after 10 h of electrochemical cultivation at the electrode potential of +0.2 V, and once the current production reached a maximum around ~9 μA cm^{-2}, it started to fall and reached minimum after few hours, which was most likely attributable to the deficiency of electron donor, lactate. Given the hydrogen sulphide generated by *D. vulgaris* Hildenborough readily reacts with Fe^{2+} precipitating iron sulphides ($HS^- + Fe^{2+} \rightarrow FeS + H^+$), the reactor medium turned black along with active metabolic current generation [31]. During the initial 10 hours, the bacteria require time to settle and grow on the anode surface. This subsequently cause the initial time delay in microbial current generation.

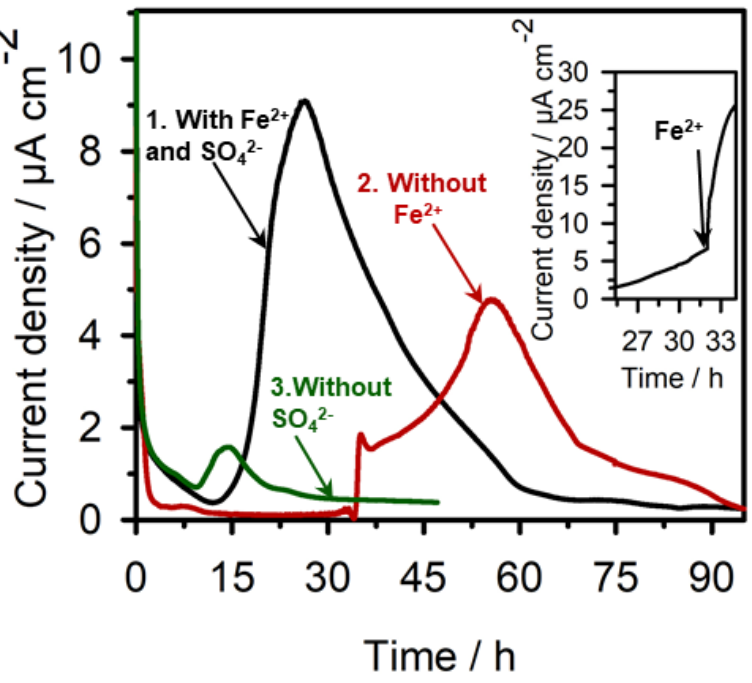


Figure 3-1 Representative anodic current generation data versus time by washed (trace 1) *D. vulgaris* Hildenborough grown on an ITO electrode at +0.2 V vs Ag/AgCl (Sat. KCl) in the presence of 1.8 mM Fe^{2+}, 17 mM sulphate, and 20 mM lactate; current generation by washed *D. vulgaris* Hildenborough cultures lacking iron (trace 2) or sulphate sources (trace 3). Inset: Effect on *D. vulgaris* Hildenborough metabolic current generation when further 1.8 mM of Fe^{2+} was added to EC reactor with unmodified medium. Arrow indicates the time point of Fe^{2+} addition.

The SEM observations on the ITO surface revealed wide distribution of *D. vulgaris* Hildenborough cells associated with iron sulphides (a, b of Figure 3-2). Elemental mapping using EDX Spectroscopy confirmed that iron sulphides were distributed throughout the ITO surface as clusters (c, d of Figure 3-2). Along with FeS clusters, spherical shaped agglomerates were also seen throughout the ITO electrodes. From elemental mapping, it was found that these spherical agglomerates had more sulphur when compared with other areas. This was most likely due to hydrogen sulphides oxidation at the anode surfaces to form elemental sulphur [32].

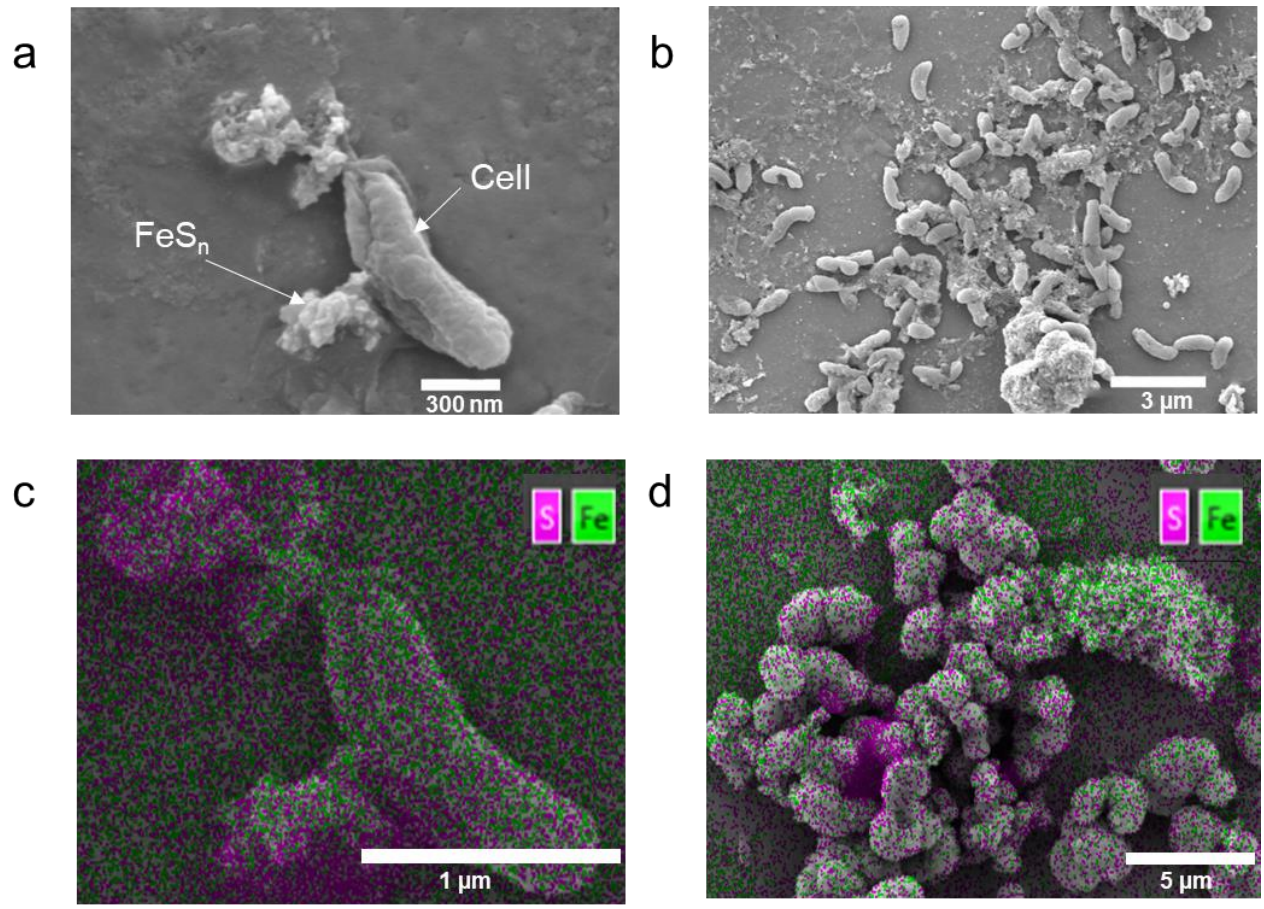


Figure 3-2. SEM (a & b) and EDX elemental mapping (c & d) of *D. vulgaris* Hildenborough cells associated with biogenic FeS_n particles obtained after 50 h of cultivation.

To examine the contribution of the biomineralization of iron sulphides on the sharp current increase, we performed the same experiments in the absence of ferrous ion or sulphate as shown in (Trace 2 & Trace 3 of Figure 3-1, respectively). As expected, considerable decrease in the anodic current generation was observed in the absence of Fe^{2+}, where sulphide production from sulphate by SRB occurred. The anodic current generation was not observed for initial few hours and then there was a sharp rise after 34 h of cultivation which then saturated and continued to grow gradually to a maximum around 4.8 µA cm^{-2}, approximately twice less than the maximum current value shown in Trace 1 in Figure 3-1. Because the formation of black FeS precipitates was not observed during the course of current generation, the results indicated that the absence of FeS decreased the rate of anodic reaction at the beginning stages. The sudden current rise may be assignable with the depletion of other electron acceptors such as contaminated oxygen in the

system, and the current generation in the latter part could be coupled with the oxidation of hydrogen sulphide at anodes [32]. The observation that the addition of 1.8 mM of Fe^{2+} after few hours of anodic current generation significantly caused a gradual increase to the anodic current with peak current, reaching as high as 26 μA cm^{-2} in two hours (Figure 3-1 inset) affirmed the positive correlation of Fe^{2+} concentration with increase in current production. Since, FeS formation was almost instantaneous [33], the gradual current increase after the Fe^{2+} addition suggest that the iron sulphides are not just abiotically oxidized at the surface of electrode but may associate with biological processes in SRB. We also confirmed the small contribution of ferrous ion on the current production with a modified medium lacking sulphate sources. Trace 3 in Figure 3-1 indicated that there was no significant metabolic current generated without sulphates. The small current observed could be attributed to the sulphates from the preculture condition. However, the current generation increased, when sulphate was added, associated with the formation of black precipitate (Figure 3-3 trace 2). Thus, these results indicated that the biomineralized iron sulphides enhanced current production of *D. vulgaris* Hildenborough at anodic conditions compared with the sulphide ion oxidation.

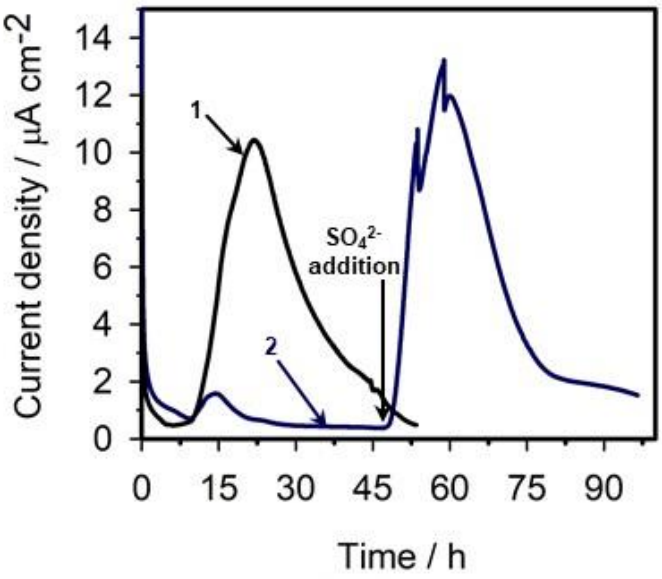


Figure 3-3. Representative anodic current generation versus time measurements by washed *D. vulgaris* Hildenborough grown on an ITO electrode in the presence of 1.8 mM Fe^{2+}, 17 mM sulphate, and 20 mM lactate (trace 1). Effect of sulphate addition on current generation by washed

D. vulgaris Hildenborough culture grown at sulphate limiting conditions (trace 2). Arrow indicate the time point at which the sulphate was added.

3.2.2. FeS mediates electron transport from metabolic lactate oxidation to the electrode

To confirm the correlation of the current production with the amount of FeS on the surface of electrode, we performed LSV before and after the sharp current increase. We observed the appearance of large anodic peak at -70 mV after the sharp current increase at 24 h, while this anodic peak current was not observed at 4 h (Figure 3-4). The anodic peak current observed at -70 mV is consistent with the potential of the FeS oxidation reaction with our observation with chemically synthesized FeS by adding sodium sulphide (Na_2S) and Fe^{2+} in the absence of *D. vulgaris* Hildenborough (Figure 3-5). In accordance with these LSV data, the synthesis of black precipitated after the initiation of sharp current increase at around 15 h in Figure 3-4 inset. These results further support our model that the biosynthesis of FeS associated with sharp current increase in *D. vulgaris* Hildenborough. However, while the anodic current at 44 h decreased to 50% from that at 24 h, the anodic peak current for FeS in LSV were almost negligible at 44 h (Figure 3-4), suggesting that FeS was oxidized after lactate depletion and did not involve in I_c at 44 h. A recovery in the anodic current but not in the FeS oxidation current was observed with the addition of lactate after the depletion of anodic current. These results indicate that iron sulphide species were formed during the sharp current increase by using lactate as electron source and oxidized by the anode surfaces after lactate deficiency [34,35].

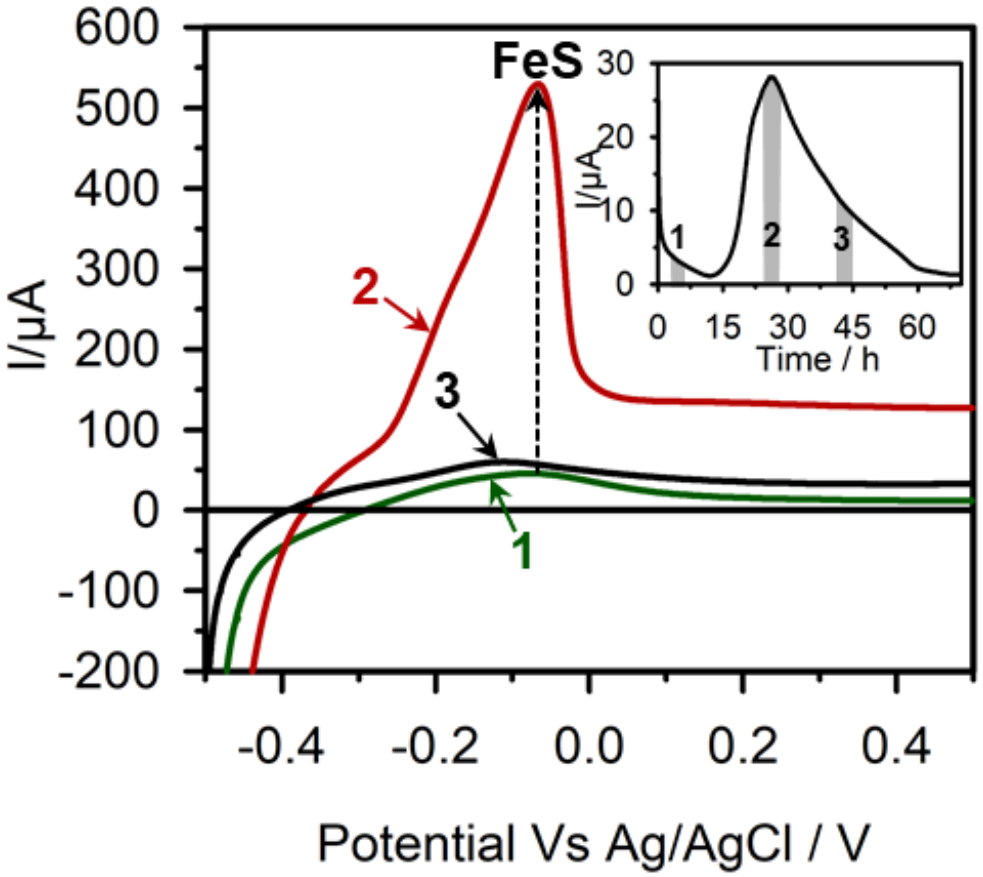


Figure 3-4. LSVs for washed SRB in EC reactor with all sources conducted after 4 h (trace 1), 24 h (trace 2) and 44 h (trace 3) of cultivation. The inset shows the representative anodic current generation by *D. vulgaris* Hildenborough at different time points.

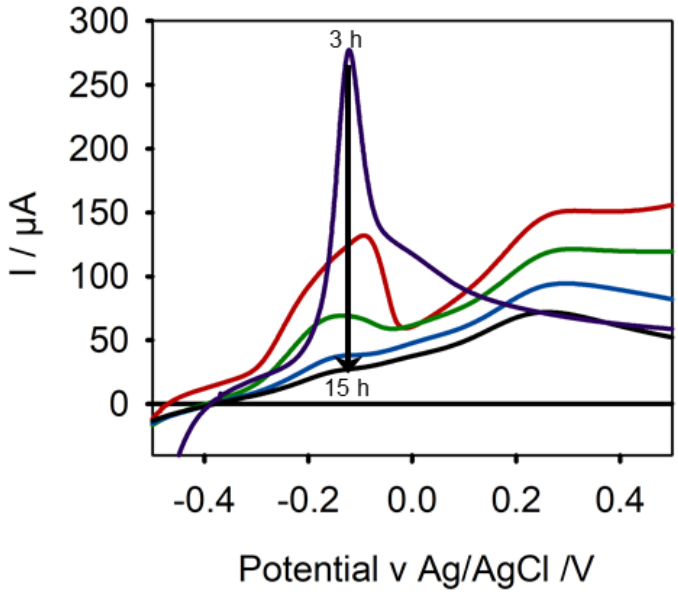


Figure 3-5. LSVs for electrochemical system inside anaerobic chamber without SRB containing chemically synthesized iron sulphides taken at every three hours interval.

To confirm that the FeS receives electrons from metabolic lactate oxidation, we next performed XPS to examine the electronic states of Fe species on the ITO electrode before and after the lactate depletion. Figure 4a and b shows Fe2p XPS spectra for ITO electrode surface in the SRB system measured after 24 h and 48 h of cultivation, respectively. The data showed that along with FeS oxidized products like FeS_2, Fe_3O_4 and Fe_2O_3 were also present on the ITO electrode surface at both time points. The Fe $2p_{3/2}$ broad peaks at 712.6 eV and 708.6 eV were assigned to FeS and FeS_2, respectively[35]. The $2p_{3/2}$ singlet at 710.9eV was attributed to Fe_2O_3 and Fe$2p_{3/2}$ peak at 708.2 eV was assigned to signals from Fe_3O_4[36,37]. The area percentage of FeS species decreased by approximately 40% after 48 h when compared to that of 24 h, suggesting that the FeS species was oxidized on the electrode surface after lactate depletion. Accordingly, the area ratio of FeS_2, Fe_3O_4 and Fe_2O_3 peaks with respect to that of FeS peak for the samples taken at 24 h, 0.08, 0.31 and 0.41, were considerably increased to 2.86, 0.35 and 0.5 in 48 h sample. This signified that lactate depletion causes the production of FeS_2 and Fe_xO_y species, more oxidative than FeS [34,35,38], demonstrating that SRB transport electron generated from metabolic lactate oxidation to the FeS.

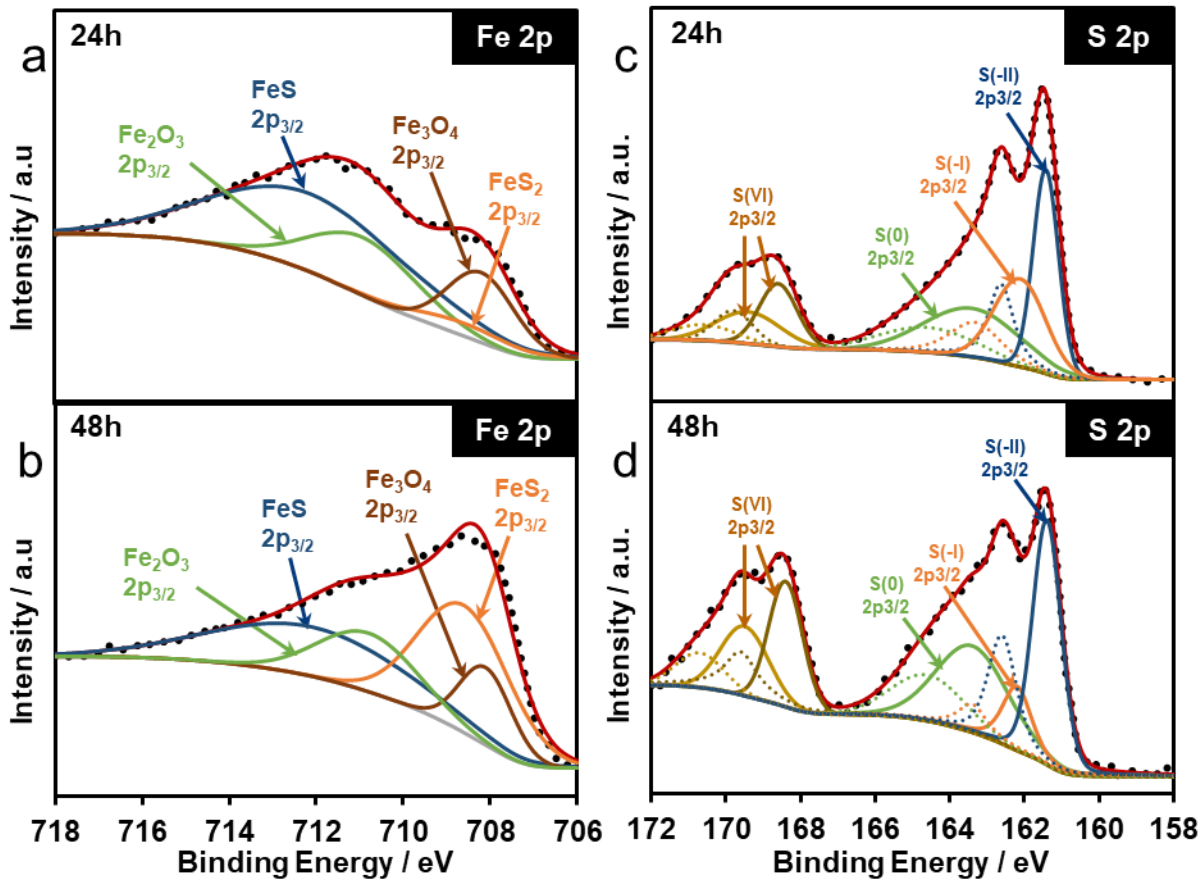


Figure 3-6. XPS Fe 2p spectrum (a & b) and S 2p spectrum (c & d) for SRB biofilms grown on ITO electrodes taken after 24 h and 48 h of cultivation; The dotted lines in c & d represents the S $2p_{1/2}$ peaks of the respective S $2p_{3/2}$ split orbitals.

3.2.3. The mechanical insight of FeS-mediated current production

To get insight into the electron transport pathway from the lactate oxidation metabolism of SRB to FeS, we examined the current production by using a mutant strain of *D. vulgaris* Hildenborough, C-cytochrome mutants (Δ*cycA*), lacking periplasmic cytochrome c3 (DVU3171) which is involved in electron transfer across the periplasm [39]. The Δ*cycA* mutant showed the peak current production considerably less than wild type (Figure 3-7). However, the current started to increase as early as wild type, which is distinct from sulphide-mediated current production, indicating that deletion of periplasmic cytochrome c3 did not totally inactivate the mechanism of FeS-mediated electron transport mechanism. Therefore, the periplasmic *C*-cytochromes may not

be the main pathway bridging the metabolism and the extracellular FeS in *D.vulgaris* Hildenborough. The less current production in the mutant strain may be due to slower production of FeS precipitates in the Δ*cycA* strain than wildtype. The alternative mechanism for electron pathway to the FeS surface would be other electron transport enzyme or even hydrogen sulphide.

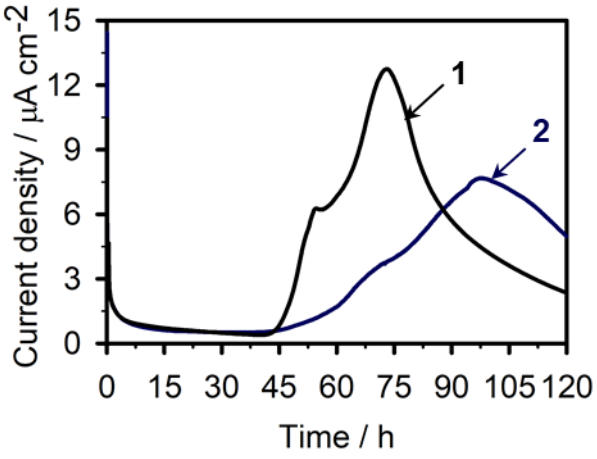


Figure 3-7. Anodic current generation versus time measurements by wild type *D. vulgaris* Hildenborough (trace 1) and Δ*cycA* mutant (trace 2) grown on an ITO electrode in the presence of 1.8 mM Fe^{2+}, 17 mM sulphate, and 20 mM lactate inside anaerobic chamber.

However, the presence of FeS clearly enhanced the current production, suggesting that the electron transport may be mediated by faster kinetics than diffusion of sulphide in extracellular process. Similar electron transport kinetics comparison has been discussed in *Shewanella ondeidensis* MR-1[40], which has outer membrane cytochromes as diffusion-less electron transport conduit to the surface of electrode. Taken together, FeS mediates electron transport by faster kinetics than sulphide diffusion process, which may suggest that SRB has alternative direct electron transport pathway than outer membrane cytochromes. Earlier reports showed that SRB can utilize metallic nanoparticles for extracellular electron transfer.[46] Our proposed mechanism for anodic current generation by *Desulfovibrio vulgaris* Hildenborough is shown in Figure 3-8.

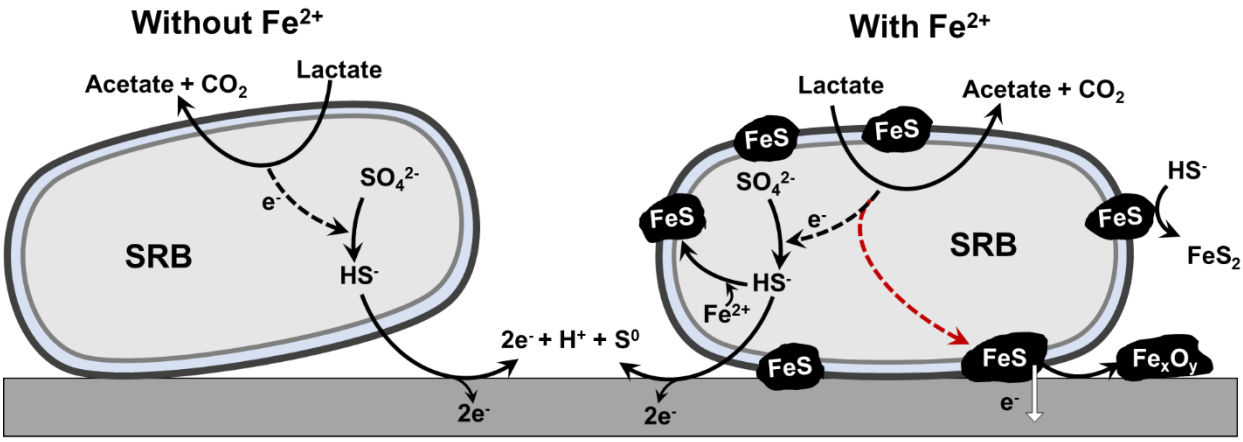


Figure 3-8. Schematic figure for proposed iron sulphide and hydrogen sulphide mediated EET in *D. vulgaris* Hildenborough.

3.2.4. Sulphide oxidation coupled anodic current generation

Metabolic current was observed in *D. vulgaris* Hildenborough EC system without FeS precipitates only when they had sulphate, suggesting the potency of sulphate derived hydrogen sulphides as an electron mediator. Upon the addition of 1.8 mM Fe^{2+}, there was almost 86% drop in anodic peak current as Fe^{2+} reacted with the hydrogen sulphide to form FeS precipitates. Then, there was an increase in current which peaked at 8 µA cm^{-2} and then gradually declined soon to be followed by a steep increase in anodic current that peaked at 23 µA cm^{-2} (Figure 3-9), which was similar to the steep current increase as seen with the control experiments lacking Fe^{2+}. The larger and later anodic current increase may be attributable to other mechanism, which is most likely the electrode oxidation of hydrogen sulphide.

Finding the electronic state of sulphur is highly important to understand the sulphide mediated reactions happening on ITO electrode surface. As shown in Figure 3-6 (c) and (d), the region of spectrum (155 – 175 eV) has sulphur transition states. The S2*p* spectra for the samples were fit with $2p_{3/2}$ and $2p_{1/2}$ doublets which were separated by a spin-orbital splitting of 1.2eV where the area ratio of $2p_{3/2}$ and $2p_{1/2}$ were set at 2:1 with identical full width at half maximum (FWHM) values[41]. The spectrum showed peaks caused by sulphates at the binding energy of 169.5 eV and 168.4 eV which can be assigned to $2p_{3/2}$ and $2p_{3/2}$ S (IV) forms for $CaSO_4$ and $MgSO_4$, respectively [42,43]. The S2$p_{3/2}$ singlet at 163.4 eV was attributed to elemental sulphur [S (0)][35]. The

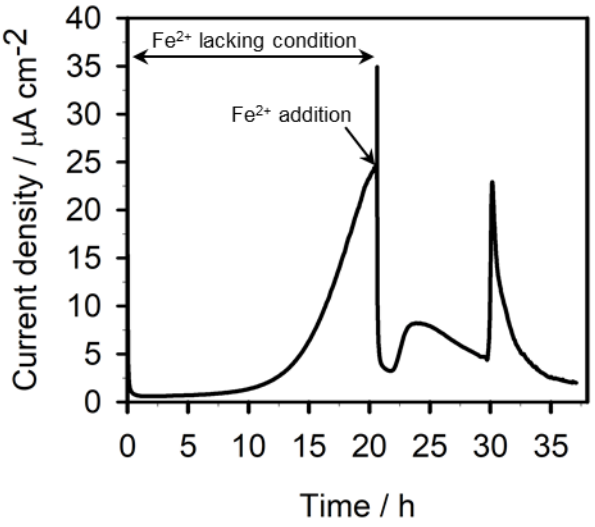


Figure 3-9 Effect of Fe^{2+} addition on *D. vulgaris* Hildenborough anodic current generation in a system which initially lacked Fe^{2+}. Prior to this experiment biofilms of *D. vulgaris* Hildenborough was formed on the ITO electrodes with an unwashed *D.vulgaris* Hildenborough culture in an unmodified reactor medium.

S2$p_{3/2}$ peaks at 162.2 eV and 161.4 eV were attributed to disulphide [S(-I)] and monosulphide [S(-II)] forms of sulphur, respectively[35,41,44]. Thus, the XPS spectrum showed that, along with sulphates, other forms of sulphur species with different electronic states were also present on the electrode surface. Accumulation of the oxidized disulphide species [S(I)] with time was observed with a rise in the ratio of S(-II) species with respect to S(-I) in the 48 h sample. The presence of S (0) supports the model that hydrogen sulphides were oxidized at anode to give elemental Sulphur according to the following equation.

$$HS^- \rightarrow S_0\downarrow + H^+ + 2 \qquad (1)$$

This anodic oxidation of sulfide has a lot of significance, if there are no other electron acceptors available to ensure its conversion to S^0, because sulphide formation is known as toxic and harmful to bacteria. For instance, nitrate is used as electron acceptor for denitrifying sulphide removal [45]. However, anode can be an excellent electron acceptor, which aid in converting the HS^- to S^0 abiotically or biotically [4,32].

3.2.5. Comparison of SRB mediated anodic current with IRB

The current density of the *D. vulgaris* Hildenborough was obtained around 9 µA / cm^2. However previous studies showed that current density in the IRB Shewanella oneidensis MR-1 showed a much lower current density at 1.75 µA / cm^2. [26] This showed that SRB pure cultures can alone contribute more anodic current than the IRBs. Thus, SRB even though consume limited organic donors for FeS precipitation by sulphate reduction, the current density at SMFCs may not have been suppressed by SRB activity.

3.3 Conclusion

The role of biomineralized iron sulphides as an electron conduit for the transfer of electrons to extracellular anodes could be possible in the marine proteobacteria *D. vulgaris* Hildenborough. The oxidative loss of iron sulphides was counterbalanced by the sulphide oxidation coupled anodic current generation. The unified electron transport model for electron transfer to external electrodes at anodic condition by the SRB *D. vulgaris* Hildenborough is proposed in this study. The possibility of FeS mediated electron transfer to the anodes in the SRB system lacking OM *c*-Cyts opened up new gates to explain or even improve the performance of SRB MFCs. Further understanding the FeS mediated anodic current generation, identification of critical enzyme in electron transport pathway, could be essential for increasing the power output of SRB MFCs performing at sulphidic environments. The higher current densities at SRB showed that, the SRB activity might not suppress the SMFC current generation

References

1. Ishii, S.; Suzuki, S.; Norden-Krichmar, T. M.; Tenney, A.; Chain, P. S. G.; Scholz, M. B.; Nealson, K. H.; Bretschger, O. A Novel Metatranscriptomic Approach to Identify Gene Expression Dynamics during Extracellular Electron Transfer. *Nat. Commun.* **2013**, *4*, 1–10.
2. Sangcharoen, A.; Niyom, W.; Suwannasilp, B. B. A Microbial Fuel Cell Treating Organic Wastewater Containing High Sulfate under Continuous Operation: Performance and Microbial Community. *Process Biochem.* **2015**, *50* (10), 1648–1655.
3. Chou, T. Y.; Whiteley, C. G.; Lee, D. J.; Liao, Q. Control of Dual-Chambered Microbial Fuel Cell by Anodic Potential: Implications with Sulfate Reducing Bacteria. *Int. J. Hydrogen Energy* **2013**, *38* (35), 15580–15589.
4. Rabaey, K.; Van de Sompel, K.; Maignien, L.; Boon, N.; Aelterman, P.; Clauwaert, P.; De Schamphelaire, L.; Pham, H. T.; Vermeulen, J.; Verhaege, M.; et al. Microbial Fuel Cells for Sulfide Removal. *Env. Sci Technol* **2006**, *40* (17), 5218–5224.
5. Sun, M.; Tong, Z.-H.; Sheng, G.-P.; Chen, Y.-Z.; Zhang, F.; Mu, Z.-X.; Wang, H.-L.; Zeng, R. J.; Liu, X.-W.; Yu, H.-Q.; et al. Microbial Communities Involved in Electricity Generation from Sulfide Oxidation in a Microbial Fuel Cell. *Biosens. Bioelectron.* **2010**, *26*, 470–476.
6. Zhao, F.; Rahunen, N.; Varcoe, J. R.; Chandra, A.; Avignone-Rossa, C.; Thumser, A. E.; Slade, R. C. T. Activated Carbon Cloth as Anode for Sulfate Removal in a Microbial Fuel Cell. *Environ. Sci. Technol.* **2008**, *42* (13), 4971–4976.
7. Habermann, W.; Pommer, E. H. Biological Fuel Cells with Sulphide Storage Capacity. *Appl. Microbiol. Biotechnol.* **1991**, *35*, 128–133.
8. Zhang, B.; Zhao, H.; Shi, C.; Zhou, S.; Ni, J. Simultaneous Removal of Sulfide and Organics with Vanadium(V) Reduction in Microbial Fuel Cells. *J. Chem. Technol. Biotechnol.* **2009**, *84*, 1780–1786.
9. Lee, D. J.; Lee, C. Y.; Chang, J. S. Treatment and Electricity Harvesting from Sulfate/Sulfide-Containing Wastewaters Using Microbial Fuel Cell with Enriched Sulfate-Reducing Mixed Culture. *J. Hazard. Mater.* **2012**, *243*, 67–72.
10. Miran, W.; Jang, J.; Nawaz, M.; Shahzad, A.; Jeong, S. E.; Jeon, C. O.; Lee, D. S. Mixed

Sulfate-Reducing Bacteria-Enriched Microbial Fuel Cells for the Treatment of Wastewater Containing Copper. *Chemosphere* **2017**, *189*, 134–142.

11. Deng, X.; Dohmae, N.; Nealson, K. H.; Hashimoto, K.; Okamoto, A. Multi-Heme Cytochromes Provide a Pathway for Survival in Energy-Limited Environments. *Sci. Adv.* **2018**, *4* (2), 1–9.
12. Dinh, H. T.; Kuever, J.; Mußmann, M.; Hassel, A. W.; Stratmann, M.; Widdel, F. Iron Corrosion by Novel Anaerobic Microorganisms. *Nature* **2004**, *427* (6977), 829–832.
13. Widdel, F.; Bak, F. Gram-Negative Mesophilic Sulfate-Reducing Bacteria. In *The Prokaryotes: A Handbook on the Biology of Bacteria: Ecophysiology, Isolation, Identification, Applications*; Balows, A., Trüper, H. G., Dworkin, M., Harder, W., Schleifer, K.-H., Eds.; Springer New York: New York, NY, 1992; pp 3352–3378.
14. Muyzer, G.; Stams, A. J. M. The Ecology and Biotechnology of Sulphate-Reducing Bacteria. *Nat. Rev. - Microbiol.* **2008**, *6* (june), 441–454.
15. Pfennig, N.; Widdel, F.; Trüper, H. G. The Dissimilatory Sulfate-Reducing Bacteria. In *The Prokaryotes: A Handbook on Habitats, Isolation, and Identification of Bacteria*; Starr, M. P., Stolp, H., Trüper, H. G., Balows, A., Schlegel, H. G., Eds.; Springer Berlin Heidelberg: Berlin, Heidelberg, 1981; pp 926–940.
16. Rickard, D.; Schoonen Martin, A. A.; Luther, G. W. Chemistry of Iron Sulfides in Sedimentary Environments. In *Geochemical Transformations of Sedimentary Sulfur*; ACS Publications, 1995; Vol. 612, pp 168–193.
17. Morse, J. W.; Cornwell, J. C. Analysis and Distribution of Iron Sulfide Minerals in Recent Anoxic Marine Sediments. *Mar. Chem.* **1987**, *22* (1), 55–69.
18. Nakamura, R.; Takashima, T.; Kato, S.; Takai, K.; Yamamoto, M.; Hashimoto, K. Electrical Current Generation across a Black Smoker Chimney. *Angew. Chemie Int. Ed.* **2010**, *49* (42), 7692–7694.
19. Yamamoto, M.; Nakamura, R.; Oguri, K.; Kawagucci, S.; Suzuki, K.; Hashimoto, K.; Takai, K. Generation of Electricity and Illumination by an Environmental Fuel Cell in Deep-Sea Hydrothermal Vents. *Angew. Chemie Int. Ed.* **2013**, *52* (41), 10758–10761.
20. Pearce, C. I. Electrical and Magnetic Properties of Sulfides. *Rev. Mineral. Geochemistry* **2006**, *61* (1), 127–180.
21. Nakamura, R.; Okamoto, A.; Tajima, N.; Newton, G. J.; Kai, F.; Takashima, T.; Hashimoto,

K. Biological Iron-Monosulfide Production for Efficient Electricity Harvesting from a Deep-Sea Metal-Reducing Bacterium. *ChemBioChem* **2010**, *11* (5), 643–645.

22. Ntarlagiannis, D.; Williams, K. H.; Slater, L.; Hubbard, S. Low-Frequency Electrical Response to Microbial Induced Sulfide Precipitation. *J. Geophys. Res. Biogeosciences* **2005**, *110* (G2), 1–12.
23. Revil, A.; Mendonça, C. A.; Atekwana, E. A.; Kulessa, B.; Hubbard, S. S.; Bohlen, K. J. Understanding Biogeobatteries: Where Geophysics Meets Microbiology. *J. Geophys. Res. Biogeosciences* **2010**, *115* (G1), 1–22.
24. Malvankar, N. S.; King, G. M.; Lovley, D. R. Centimeter-Long Electron Transport in Marine Sediments via Conductive Minerals. *Isme J.* **2014**, *9*, 527–531.
25. Wu, X.; Zhao, F.; Rahunen, N.; Varcoe, J. R.; Avignone-Rossa, C.; Thumser, A. E.; Slade, R. C. T. A Role for Microbial Palladium Nanoparticles in Extracellular Electron Transfer. *Angew. Chemie - Int. Ed.* **2011**, *50* (2), 427–430.
26. Kondo, K.; Okamoto, A.; Hashimoto, K.; Nakamura, R. Sulfur-Mediated Electron Shuttling Sustains Microbial Long-Distance Extracellular Electron Transfer with the Aid of Metallic Iron Sulfides. *Langmuir* **2015**, *31* (26), 7427–7434.
27. Torres, C. I.; Marcus, A. K.; Lee, H. S.; Parameswaran, P.; Krajmalnik-Brown, R.; Rittmann, B. E. A Kinetic Perspective on Extracellular Electron Transfer by Anode-Respiring Bacteria. *FEMS Microbiol. Rev.* **2010**, *34*, 3–17.
28. Heidelberg, J. F.; Seshadri, R.; Haveman, S. A.; Hemme, C. L.; Paulsen, I. T.; Kolonay, J. F.; Eisen, J. A.; Ward, N.; Methe, B.; Brinkac, L. M.; et al. The Genome Sequence of the Anaerobic, Sulfate-Reducing Bacterium Desulfovibrio Vulgaris Hildenborough. *Nat. Biotechnol.* **2004**, *22* (5), 554–559.
29. Sim, M. S.; Wang, D. T.; Zane, G. M.; Wall, J. D.; Bosak, T.; Ono, S. Fractionation of Sulfur Isotopes by Desulfovibrio Vulgaris Mutants Lacking Hydrogenases or Type I Tetraheme Cytochrome C3. *Front. Microbiol.* **2013**, *4* (JUN), 1–10.
30. Saito, J.; Hashimoto, K.; Okamoto, A. Flavin as an Indicator of the Rate-Limiting Factor for Microbial Current Production in Shewanella Oneidensis MR-1. *Electrochim. Acta* **2016**, *216* (September), 261–265.
31. Zhou, C.; Vannela, R.; Hayes, K. F.; Rittmann, B. E. Effect of Growth Conditions on Microbial Activity and Iron-Sulfide Production by Desulfovibrio Vulgaris. *J. Hazard.*

Mater. **2014**, *272*, 28–35.

32. Sun, M.; Mu, Z. X.; Chen, Y. P.; Sheng, G. P.; Liu, X. W.; Chen, Y. Z.; Zhao, Y.; Wang, H. L.; Yu, H. Q.; Wei, L.; et al. Microbe-Assisted Sulfide Oxidation in the Anode of a Microbial Fuel Cell. *Environ. Sci. Technol.* **2009**, *43* (9), 3372–3377.
33. Rickard, D. Experimental Concentration-Time Curves for the Iron(II) Sulphide Precipitation Process in Aqueous Solutions and Their Interpretation. *Chem. Geol.* **1989**, *78* (3), 315–324.
34. Boursiquot, S.; Mullet, M.; Abdelmoula, M.; Génin, J.-M.; Ehrhardt, J.-J. The Dry Oxidation of Tetragonal FeS1- x Mackinawite. *Phys. Chem. Miner.* **2001**, *28* (9), 600–611.
35. Dong, C.; Zheng, X.; Huang, B.; Lu, M. Enhanced Electrochemical Performance of FeS Coated by Ag as Anode for Lithium-Ion Batteries. *Appl. Surf. Sci.* **2013**, *265*, 114–119.
36. McIntyre, N. S.; Zetaruk, D. G. X-Ray Photoelectron Spectroscopic Studies of Iron Oxides. *Anal. Chem.* **1977**, *49* (11), 1521–1529.
37. Panzmer, G.; Egert, B. The Bonding State of Sulfur Segregated to α-Iron Surfaces and on Iron Sulfide Surfaces Studied by XPS, AES and ELS. *Surface Science*. 1984, pp 651–664.
38. Zhou, L.; Liu, J.; Dong, F. Spectroscopic Study on Biological Mackinawite (FeS) Synthesized by Ferric Reducing Bacteria (FRB) and Sulfate Reducing Bacteria (SRB): Implications for in-Situ Remediation of Acid Mine Drainage. *Spectrochim. Acta - Part A Mol. Biomol. Spectrosc.* **2017**, *173*, 544–548.
39. Matias, P. M.; Coelho, A. V.; Valente, F. M. A.; Plácido, D.; LeGall, J.; Xavier, A. V.; Pereira, I. A. C.; Carrondo, M. A. Sulfate Respiration in Desulfovibrio Vulgaris Hildenborough: Structure of the 16-Heme Cytochrome c HmcA at 2.5-Å Resolution and a View of Its Role in Transmembrane Electron Transfer. *J. Biol. Chem.* **2002**, *277*, 47907–47916.
40. Okamoto, A.; Hashimoto, K.; Nealson, K. H.; Nakamura, R. Rate Enhancement of Bacterial Extracellular Electron Transport Involves Bound Flavin Semiquinones. *Proc. Natl. Acad. Sci.* **2013**, *110* (19), 7856–7861.
41. Lan, Y.; Butler, E. C. Iron-Sul Fi de-Associated Products Formed during Reductive Dechlorination of Carbon Tetrachloride. **2016**.
42. Peisert, H.; Chassé, T.; Streubel, P.; Meisel, A.; Szargan, R. Relaxation Energies in XPS and XAES of Solid Sulfur Compounds. *J. Electron Spectros. Relat. Phenomena* **1994**, *68*

(C), 321–328.

43. Yu, X. R.; Liu, F.; Wang, Z. Y.; Chen, Y. Auger Parameters for Sulfur-Containing Compounds Using a Mixed Aluminum-Silver Excitation Source. *J. Electron Spectros. Relat. Phenomena* **1990**, *50* (2), 159–166.
44. Thomas, J. E.; Jones, C. F.; Skinner, W. M.; Smart, R. S. C. The Role of Surface Sulfur Species in the Inhibition of Pyrrhotite Dissolution in Acid Conditions. *Geochim. Cosmochim. Acta* **1998**, *62* (9), 1555–1565.
45. Vaiopoulou, E.; Melidis, P.; Aivasidis, A. Sulfide Removal in Wastewater from Petrochemical Industries by Autotrophic Denitrification. *Water Res.* **2005**, *39*, 4101–4109.
46. Wu, X.; Zhao, F.; Rahunen, N.; Varcoe, J. R.; Avignone‐Rossa, C.; Thumser, A. E.; Slade, R. C., A role for microbial palladium nanoparticles in extracellular electron transfer. Angewandte Chemie International Edition 2011, 50 (2), 427-430.

Chapter 4

Iron sulphide nanoclusters induced synergetic relationship between Sulphate Reducing Bacteria and Iron Reducing Bacteria coculture systems

4.1 Introduction

At marine sedimental environments, usually there is competition for limited organic electron donors for the bacterial communities. However, the IRBs and SRBs can co-exist with each other at these reductive environments and dominate the SMFC electrode surfaces which is quite unsure how these both bacteria communities interact with each other. Interactions of SRB and IRB pure cultures on anodic current generation was already reported. [1-3] In both cases, it was showed that the presence of FeS actively dominated the current generation. [1, 4] In Shewanella species, presence of FeS nanoparticles increased their overall electricity generation by 100 folds and past reports claimed for FeS based long range electron transfer with the IRB anodic current generation. In our previous study, we observed that the bioprecipitates FeS nanoclusters increased the anodic current generation in the SRB, *Desulfovibrio vulgaris* Hildenborough. However, it is quite unsure how SRB, IRB and FeS can interact with each other in the sediments and impact the overall anodic current generation by SMFCs. Since the biomineralized FeS increased the anodic current generation in both SRB and IRB individual monoculture EC systems, the SRB mediated FeS nanoclusters could involve in increasing the overall current generation by IRB. This kind of relationships could change their environment from competitive relationship to a friendly one.

In this current work, in an attempted to elucidate the SRB and IRB interactions in the presence of bio-precipitated FeS nanoclusters at SMFC anode surfaces, whole-cell electrochemical assays were performed with SRB and IRB cocultures under anodic conditions in a three-cell electrochemical system. The effect of biosynthesized FeS nanoclusters on the overall anodic current generation was performed. *Shewanella oneidensis* MR-1 and *Desulfovibrio vulgaris* Hildenborough were used as model organisms for IRB and SRB respectively. The structure of coculture agglomerates formed on the electrode surfaces were studied by making cross sectional thin sections. In order to identify the effect of FeS nanoclusters on the coculture bioagglomerates conductive properties, source-drain experiments were performed in this system with interdigitated

electrode arrays (IDA).[5] The findings showed the prevalance of FeS based long-range electron conduction in the coculture bio agglomerates.

4.2 Results and Discussion:

4.2.1 Synergetic current generation in SRB and IRB co-cultures

In order to examine the interaction between SRB and IRB on anodic current generation, their respective model bacteria, *D. vulgaris* Hildenborough and *S. oneidensis* MR-1 were added together to a three-electrode electrochemical (EC) reactor with indium tin–doped oxide (ITO) electrodes containing modified WP medium as the electrolyte. The electrolyte was supplemented with 20 mM lactate, 17 mM sulfate and 1.8 mM Fe^{2+}. We added 0.05 ml of washed *D. vulgaris* Hildenborough culture to the EC system where as the final optical density of *S. oneidensis* MR-1 was maintained at 10^{-4}_{600nm} and it was poised at +0.2 V vs Ag/AgCl (KCl Saturated) reference electrode. These low cell concentrations were derived from the low abundance of SRB and IRB at sulphidic sedimental environments. Followed by decrease and gradual rise in current production, a steep increase in the current was observed after 25 h, and reached to 70 µA (Figure 4-1). The bacteria require time to settle and start growing on the anode surface which caused the initial time delay in the current production. The electrochemical reactor medium showed black precipitates formation during active current production mostly likely generated from biomineralization of iron sulphide nanoclusters by SRB activity. Given the current production is strongly dependent on the lactate concentration, the observed current production is suggested to be coupled with microbial metabolic activity. In contrast to the coculture system, the anodic current production by *S. oneidensis* MR-1 showed a peak current of 2.5 µA which was almost 28 times lesser than the coculture anodic peak current even though coupled with black precipitate production. Also, negligible current generation and black precipitates formation were observed in the EC system having *D. vulgaris* Hildenborough pure cultures. These data showed the prevalence of a synergetic interaction between *D. vulgaris* Hildenborough and *S. oneidensis* MR-1 for anodic current generation. Also, the increase in electron donor lactate concentration increased the peak current showing the importance of electron source on the current generation (Figure 4-2).

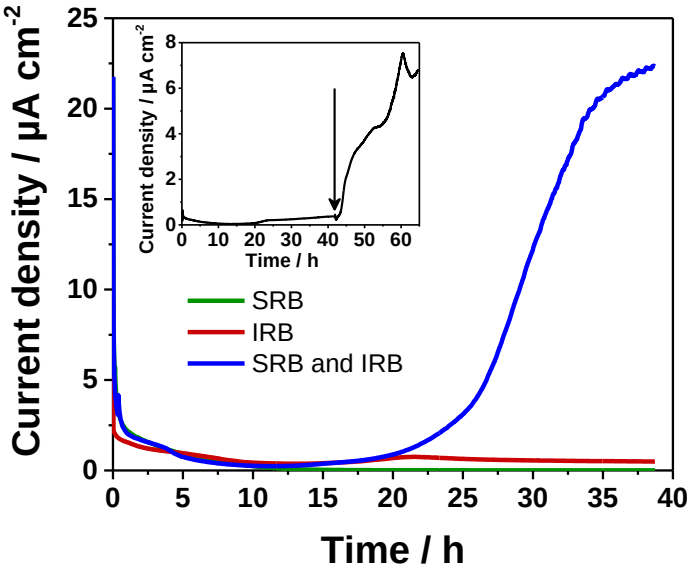


Figure 4-1 Representative anodic current generation in the electrochemical system with 20 mM Lactate as the electron donor when SRB (Green trace), IRB (Red line) and both SRB & IRB (Blue line) were added.

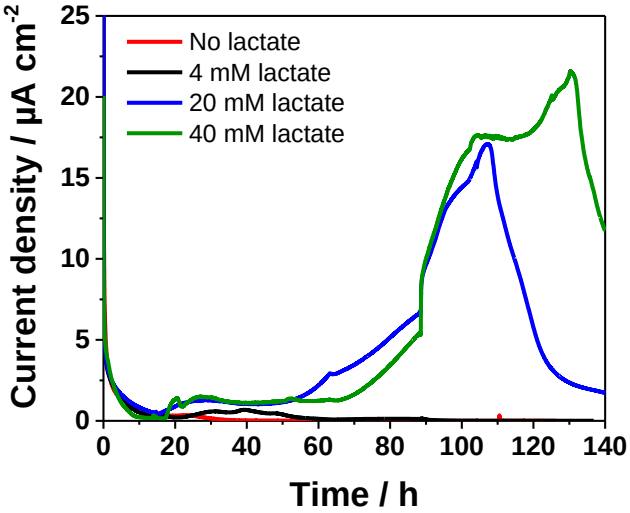


Figure 4-2 Representative anodic current generation by SRB & IRB coculture system without lactate (red line), with 4 mM lactate (black line), 20 mM lactate (blue line) and 40 mM lactate (green line) were added to the EC system

4.2.2 Iron sulphides production couples with the synergetic current production in the coculture system

Associated with the synergetic current production, black precipitate was formed and accumulated on the electrode. As sulfide would be actively produced during the current production, the black precipitate is most likely FeS. The precipitates formed on the surface of anode during active current generation was analyzed by scanning electron microscopic (SEM) studies(Figure 4-3 a). Agglomerates of bacterial cells along with the nano-sized particles was observed on the anode surface. Energy-dispersive X-ray spectroscopy (EDX) showed that these particles contained Iron and Sulphur (Figure 4-3 b), and both of these species were distributed on the surface of bacterial cells and also on the electrode surface, strongly suggesting that the black precipitation is FeS agglomerates, and nanoparticles of FeS physically associate with bacteria. Given that the iron mono sulphides in their tetragonal form shows excellent electrical conductive properties, and both *S. oneidensis* MR-1 and *D. vulgaris* Hildenborough also showed electrogenic properties, chances are that these bioagglomerates can make use of these conductive FeS nanoparticles to conduct electrons effectively across the bioagglomerates.

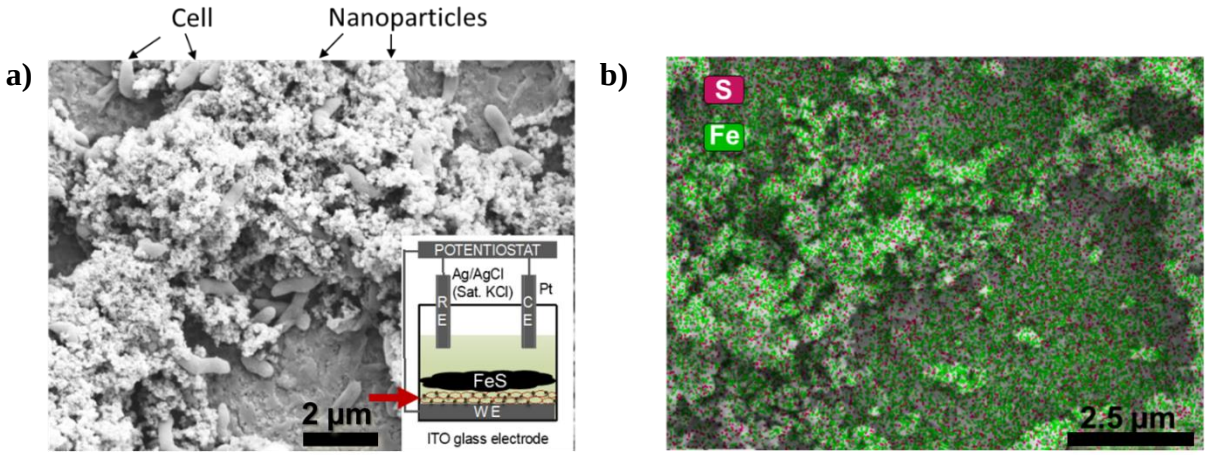


Figure 4-3 (a) Scanning Electron Microscopy observation and (b) Energy-dispersive X-ray spectroscopy of the bio agglomerates formed on the anode surface. The iron species were marked green and sulphur species were marked red. Wide distribution of both sulphur and iron species were observed.

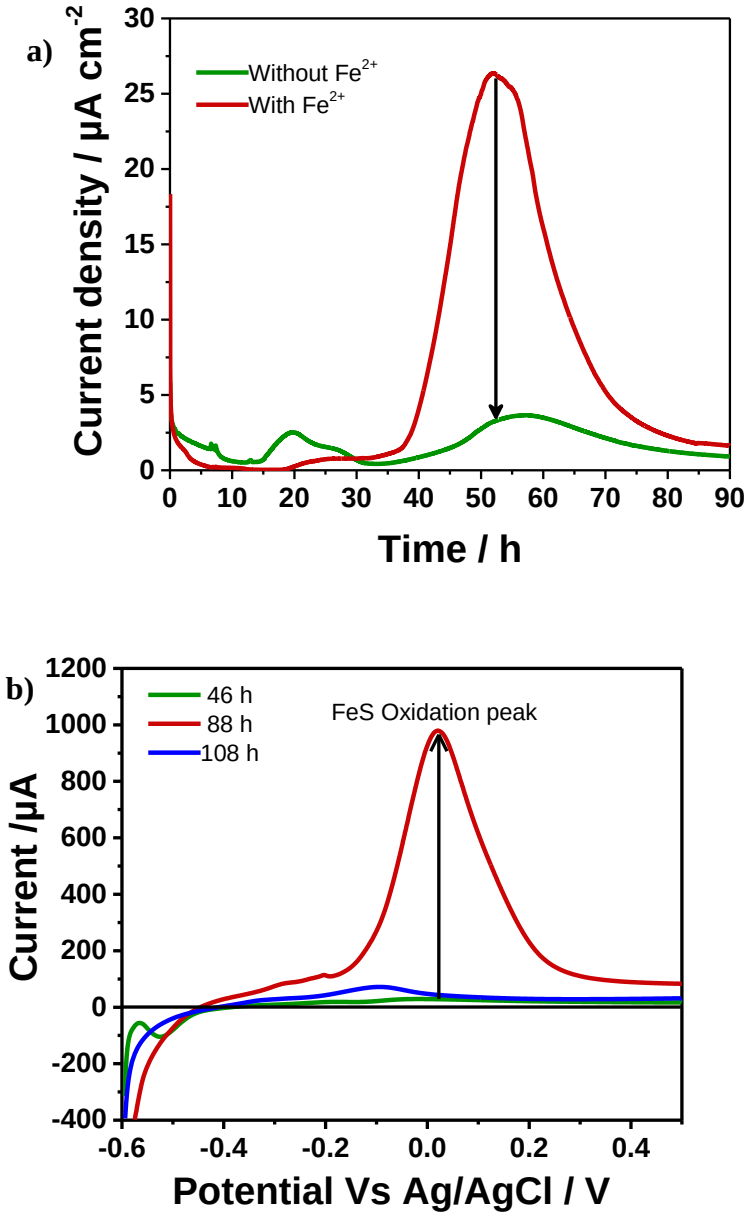


Figure 4-4 (a) Linear sweep voltagram observed at different time intervals in the SRB and IRB coculture electrochemical system (b) Representative anodic current generation showing the difference in anodic current generation by the SRB and IRB coculture system supplemented with 20 mM lactate with Fe^{2+} (red line) and without Fe^{2+} (green line).

This importance of biosynthesized FeS on the synergetic current generation was confirmed by current production measurements in the absence of Fe^{2+} with coculture system of *D. vulgaris* Hildenborough and *S. oneidensis* MR-1, to limit the formation of FeS bio-precipitates. While small current increase was observed at the initial stage at around 20 hours, the maximum current production was 80% less than that in the presence of Fe^{2+}(Figure 4-4 a). This phenomenon clearly showed that the synergetic current generation was largely dependent on the formation of FeS bio agglomeration. Linear sweep voltammetry (LSV) further demonstrated the correlation between current increase and the biosynthesis of FeS. During active synergetic current generation, when the EC reactor started showing black FeS precipitates formation, FeS oxidation peak was observed around 20mV by performing (Figure 4-4 b). In contrast, the FeS oxidation peak and the formation of black precipitates was observed neither at the initial phase of current generation nor after current depletion. Given current decrease was caused by lactate depletion and FeS formation stops after the current production decrease, the lack of oxidative current for FeS after current decrease might be caused by the oxidation of FeS at +0.4 V vs SHE. These data demonstrated that the biosynthesis of FeS was required for the synergetic current production.

4.2.3 Enhancement of conductive networks in the coculture system

Although the FeS bioagglomerate formation is required for synergetic current generation, the FeS bioagglomerates formation was also observed with *D. vulgaris* Hildenborough. Electrically conductive nanoparticles were proposed to mediate long-range electron transport of *S. oneidensis* MR-1 [4]. Therefore, MR-1 may transport electron through FeS biosynthesized by *D. vulgaris* to the electron and dominantly contribute to the current enhancement in coculture system. In order to examine this idea, we first used mutant strain lacking outermembrane cytochrome c (Δ*omcALL*) to examine the contribution of MR-1, because OM c-Cyts are known to mediate EET of MR-1(Figure 4-5). We observed that the anodic current generation was affected by using Δ*omcALL* MR-1 mutant when compared to that of the wild type MR-1. These results suggest that *S. oneidensis* MR-1 dominantly contributed the current enhancement in the coculture system.

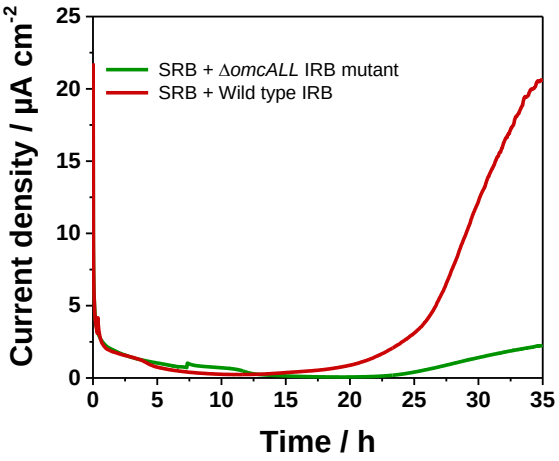


Figure 4-5 Representative anodic current generation in the coculture system when the outermembrance C-type cytochrome IRB mutant (Δ*omcALL*) and wild type SRB strains were added to the EC system

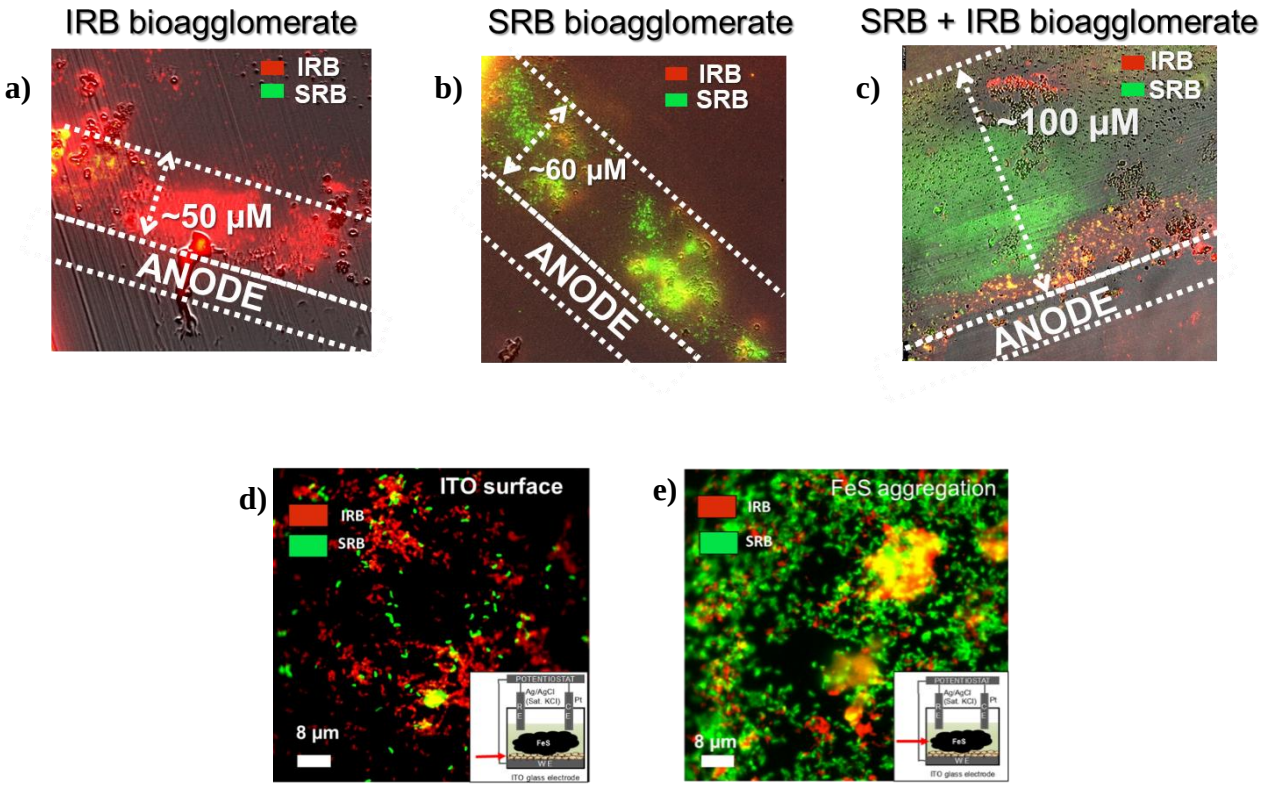


Figure 4-6 Respective Fluorescent In-situ hybridization (FISH) microscopic images of the cross-sectional thin sections of the bioagglomerates formed on the anode surface when only IRB (a), SRB (b) and IRB & IRB (c) were added to the EC system. FISH microscopic images representing the SRB and IRB distribution found on the anode surface (d) and in the FeS bioagglomerates (e) formed on the anodic surface.

We examined the localization of MR-1 in the bioagglomerate cross-section, by using respective Fluorescent In-situ hybridization (FISH) probes that particularly label SRB and IRB strains (Figure 4-6). As we expected, the IRB localized near the electrode surface, and associated with SRB. In addition, the thickness of coculture system bioagglomerate was observed to be around 100 µm compared to 60 µm and 50 µm found in pure culture systems of SRB and IRB respectively. Thus, the current observation showed formation of enhanced formation of conductive networks on the anode surfaces.

4.2.4 Need to investigate electron transfer across bioagglomerates

Since it was observed that the anodic current generation was dominated by the presence of FeS bioagglomerates, the mechanism by which how FeS increases the electron transfer to the anode surface has to be investigated. Studying the conductive properties of bioagglomerates formed on the anode surface can give insights on FeS dependent synergetic current generation. In previous studies with pure cultures of *Shewanella* species, possibility of FeS mediated long range electron transfer was mentioned. According to SEM analysis the bacterial cells were found distributed within the FeS bioagglomerates, which interests the need to check for electron transfer mechanisms across longer distances within the bioagglomerates.

4.2.5 Source-drain experiments to study the bioagglomerate conductive properties

In order to study the electron transfer across bioagglomerates, source -drain experiments were performed using interdigitated electrode arrays (IDA) with four electrode systems. Two parallel working electrodes (W.E.) each setup at 15µm apart were alternatively arranged. Electrical gradient was established across W.E. 1 and W.E. 2 by posing them with different potentials originating for source-drain potential (V_{SD}). Thus, the more negative electrode can function as

electron source and more positive electrode will function as electron drain. The resulting current flowing across these two working electrodes is the source-drain current (I_{SD}). The source drain current depends on the conductive properties of the phase adjoining the two adjacent working electrodes.[5]

The coculture bioagglomerates were first formed on the IDA electrodes before measuring I_{SD} across the bioagglomerates. Initially EC reactor was setup with the IDA electrodes where both working electrodes were set at + 0.2 V with respect to the reference electrode (Figure 4-7). Synergetic anodic current production at individual W.E.s was observed, while active FeS precipitation was also observed in the EC system. When observed under microscope it was found that the bioagglomerates formed on the IDA electrode adjoined the adjacent electrodes (Figure 4-8). Thus, a thick bioagglomerate formation joining both W.E.s was observed.

The bioagglomerates which were formed during active synergetic current generation was subjected for source-drain studies. the V_{SD} was maintained constant at 0.05 V. I_{SD} was measured at both electrodes while sweeping from 0 V to -1.0 V for W.E. 1 at a scan rate of 2.0 mV/S. The I_{SD} was observed with respect to gate potential (E_{avg}), the average between source electrode potential and drain electrode potential. When the gate potential is equal to the formal potential of the redox active species present in the bioagglomerates, the I_{SD} tends to be maximum and alternatively, there would be a drop in the current when the E_{avg} is greater or lesser than the formal potential.

4.2.6 FeS based long range electron transfer in the bioagglomerates

The I_{SD} for coculture system observed during active current generation obtained symmetrical current values across the scan range. Initially, the I_{SD} seemed to be smaller around -20 µA for both electrodes and as the E_{avg} becomes more negative the I_{SD} started to increase in both source and drain electrodes indicating the flow of electrons across the bioagglomerates which adjoin adjacent source and drain electrodes(Figure 4-9). On the reverse scan the I_{SD} decreased and reached a minimum value which can be related to oxidation of FeS. At neutral pH, the phase transition of FeS into FeS_2 and Fe_2O_3 starts around -0.650 V vs Ag/AgCl (KCl saturated).

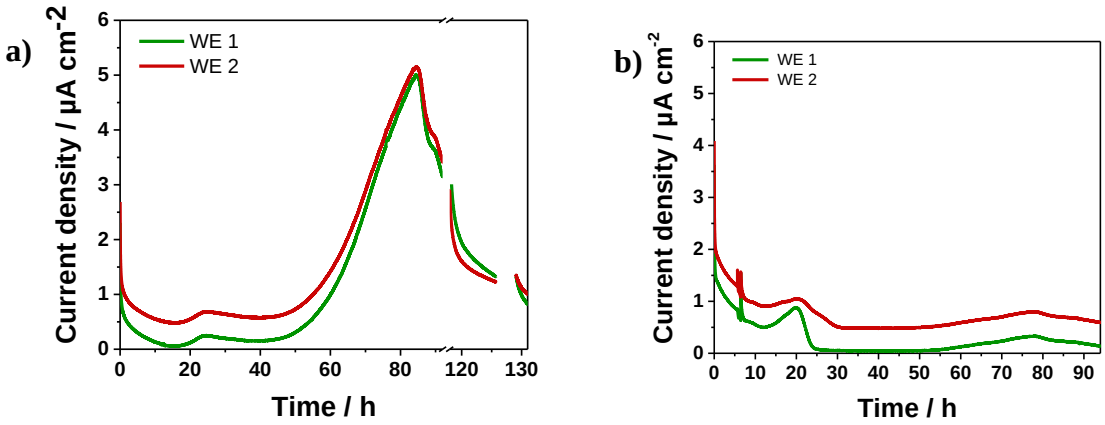


Figure 4-7 Representation anodic current generation in the SRB and IRB coculture EC system on both source and drain working electrodes when they were maintained at same potential with respect to the reference electrode in a system with Fe^{2+} (a) and without Fe^{2+} (b)

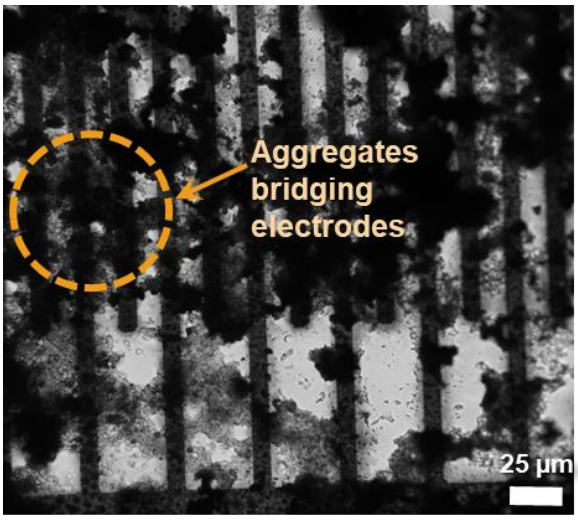


Figure 4-8 Observed bioagglomerates formed on the surface of interdigitated electrode adjoining the adjacent electrode arrays

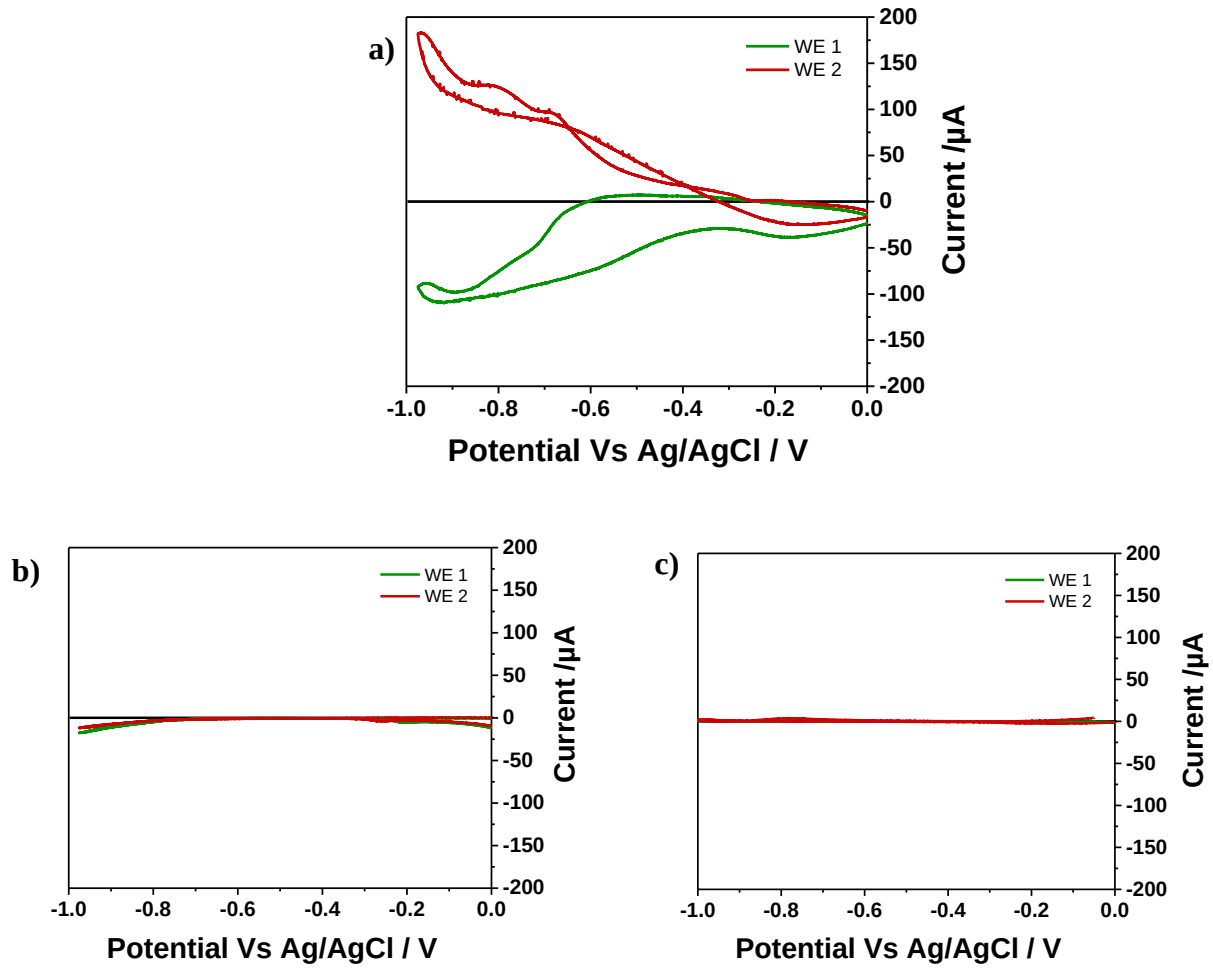


Figure 4-9 Source-drain current observed after 92 h of inoculation (a) during active FeS generation, after 131 h of inoculation (b) when most of the FeS were oxidized and source-drain current produced in the EC system without Fe^{2+} and no FeS generation measured after 94 h of inoculation (c)

This could explain rise in source current at potentials negative than -0.650 V during the forward scan from 0 V. Thus, at more negative potential, formation of FeS is favored. Also, the Fe^{2+} which is pivotal for FeS formation can also be generated by reduction of Fe^{3+} at the anode surfaces at more negative potentials. At -0.95 V the drain current was around 200 µA compared to -100 µA which was stoichiometrically 100 µA higher than the electrons donated from source electrode. This extra flux of electrons can be explained by donation of electrons to drain electrodes

by oxidation of FeS thereby increasing baseline current for drain electrodes. Since, the individual bacterial cell length is not enough to adjoin adjacent working electrodes, the electron transfer between them could happen only when they are connected by a conductive matrix. Thus, from the current flow across the source and drain electrodes, it can be pointed that long-range electron transfer is probable across the coculture bioagglomerates.

However, after current depletion where most of the FeS species were oxidized, no considerable I_{SD} was observed. This can be clearly related with depletion of I_{SD} with respect to FeS depletion. Also, the I_{SD} was not observed when measured with negative control system without Fe^{2+} further confirming the involvement of FeS precipitates for long range electron conduction across the bioagglomerates.

4.3 Conclusion

Coculture anodic current generation studies with model SRB and IRB bacteria showed that synergetic current generation was possible which is specifically dependent on the formation of FeS bio precipitates within the system. FeS based long-range electron transfer across the bioagglomerates formed on the anodic surfaces was observed. Also, formation of a thicker bioagglomerate on anode surface was observed when compared to bioagglomerates of pure culture system. Thus, increasing the bioagglomerate conductivity would also increase the performance of SMFC current generation. The FeS biosynthesis by SRB showed a positive feedback loop for increasing the overall microbial current generation on the electrodes. Involvement of other potential metal sulphides for current generation can also be developed based on the observation on the current study which poses immense potential to power devices based on SMFC.

References

1. Murugan, M.; Miran, W.; Masuda, T.; Lee, D. S.; Okamoto, A., Biosynthesized Iron Sulfide Nanocluster Enhanced Anodic Current Generation by Sulfate Reducing Bacteria in Microbial Fuel Cells. *ChemElectroChem* **2018,** *5* (24), 4015-4020.
2. Miran, W.; Jang, J.; Nawaz, M.; Shahzad, A.; Jeong, S. E.; Jeon, C. O.; Lee, D. S., Mixed sulfate-reducing bacteria-enriched microbial fuel cells for the treatment of wastewater containing copper. *Chemosphere* **2017,** *189*, 134-142.
3. Okamoto, A.; Hashimoto, K.; Nakamura, R., Long-range electron conduction of Shewanella biofilms mediated by outer membrane C-type cytochromes. *Bioelectrochemistry* **2012,** *85*, 61-5.
4. Nakamura, R.; Okamoto, A.; Tajima, N.; Newton, G.; Kai, F.; Takashima, T.; Hashimoto, K., *Biological Iron-Monosulfide Production for Efficient Electricity Harvesting from a Deep-Sea Metal-Reducing Bacterium*. 2010; Vol. 11, p 643-5.
5. Snider, R. M.; Strycharz-Glaven, S. M.; Tsoi, S. D.; Erickson, J. S.; Tender, L. M., Long-range electron transport in Geobacter sulfurreducens biofilms is redox gradient-driven. *Proc Natl Acad Sci U S A* **2012,** *109* (38), 15467-72.

Chapter 5

Iron reducing bacteria enhanced synergetic growth and iron sulphide bio precipitation in the sulphate reducing bacteria

5.1 Introduction

In the electro chemical system, it was observed that the precipitation of iron monosulphides (FeS) actively dominated the microbial electricity generation. The conductive properties of FeS helped for higher flux of electrons to the anode surface by performing long-range electron transfer across the bacterial-FeS bio agglomerated which span around 100 μm in thickness. The coculture system actively generated FeS nanoparticles during the synergetic current generation and there was no growth and FeS bio precipitation was observed in the electrochemical system with SRB pure culture system. This clearly exhibited that the SRB was benefited by the addition of IRB into the system and the IRB positively promoted the SRB activity.

In order to understand the importance on IRB on the SRB activity, it might be important to observe how these two bacteria species interact with each other in the natural systems, particularly without any applied potentials. Previous studies showed synergetic interactions between bacteria at the MFCs [1]. Recent work with SRB show that, the FeS nanoparticles which are attached with the microbial membrane can transfer electrons across the cell membrane more specifically by conducting electrons inside the SRB cells. The bacteria do it in order to survive at low energetic environments.[2] In this work the importance of IRB on the SRB activity was observed in a non-electrochemical system in order to identify their interactions at natural environments. The bacterial cultures of SRB and IRB were added inside a bottled system with the same electrolyte medium and the microbial interactions were observed. The observations showed that the presence of IRB influenced the SRB activity and FeS production inside this closed non-electrochemical system. Accelerated FeS generation by SRB was observed in the presence of IRB.

5.2 Results and Discussion:

5.2.1 Iron reducing bacteria dependent iron sulphides bio precipitation

To check the influence of IRB on the SRB mediated FeS bioprecipitation, the cells of SRB and IRB were added together inside a bottled system with of the electrolyte medium used for electrochemical experiments. The medium was supplemented with 20 mM lactate, 17 mM sulfate and 1.8 mM Fe^{2+}. We added 0.2 ml of washed *D. vulgaris* Hildenborough culture to the EC system where as the final optical density of *S. oneidensis* MR-1 was maintained at $10^{-4}_{600\ nm}$ while maintaining a final volume of 20 ml medium inside the closed bottle. The medium was maintained at anaerobic conditions and it was incubated at 30 °C throughout the experiments. Within 12 hours the formation of black FeS precipitates was observed inside the closed system and it started to precipitate more with time. The extend of black precipitation can be visually observed inside the closed bottle system and it became darker with time. Similar experiments were conducted by adding only SRB and IRB pure cultures inside the closed bottle system and the formation of black precipitates were observed.

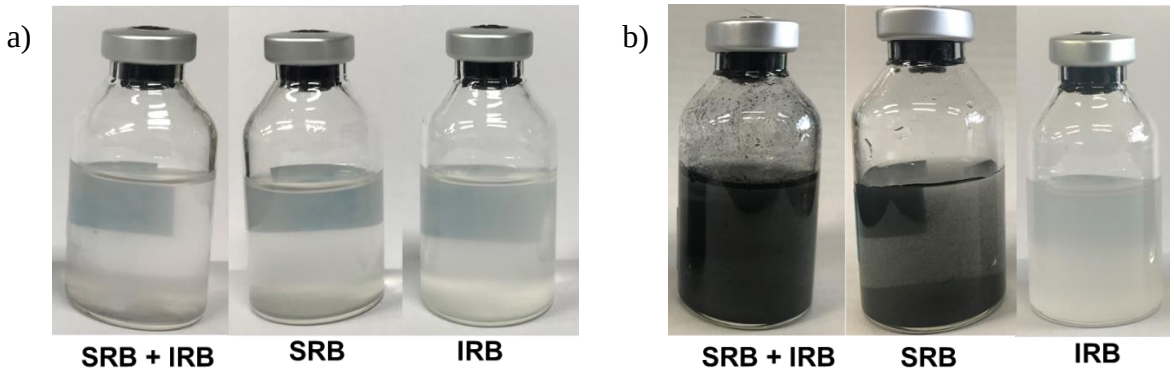


Figure 5-1 Representative observations of the precipitation of black FeS nanoparticles in the bottled system having 20mM lactate, 17 mM sulfate and 1.8 mM Fe^{2+} when SRB and IRB, SRB and IRB were added. (a) and (b) represents observations after 3 hours and 24 hours of incubation respectively.

It was observed that the formation of black FeS precipitates were accelerated inside the closed coculture system. From the Figure 5-1(b) it was clear that there were blacker FeS precipitated in the coculture system compared to that of SRB pure cultures after 24 hours of incubation. FeS precipitation was not observed inside the system wit only IRB confirming that IRB is not possible to precipitate FeS in the presence of sulphates. Similar observations were seen in multiple experiments which confirmed that the presence of IRB has accelerated the FeS precipitation inside the bottled system even without any electrodes. This explains potential microbial interactions that might be happening at the sedimental sub surfaces.

5.2.2 Accelerated microbial activity inside the cocultures

Since the visual observations showed that the FeS acceleration was increased in the presence of IRB, we tried to quantify the precipitates formed inside the system. The quantity of the bioprecipitates formed inside the system was calculated by centrifuging the medium collected from the bottles after the experiments and then weighed to quantify the agglomerates. This will compose both FeS precipitates and microbial biomass.

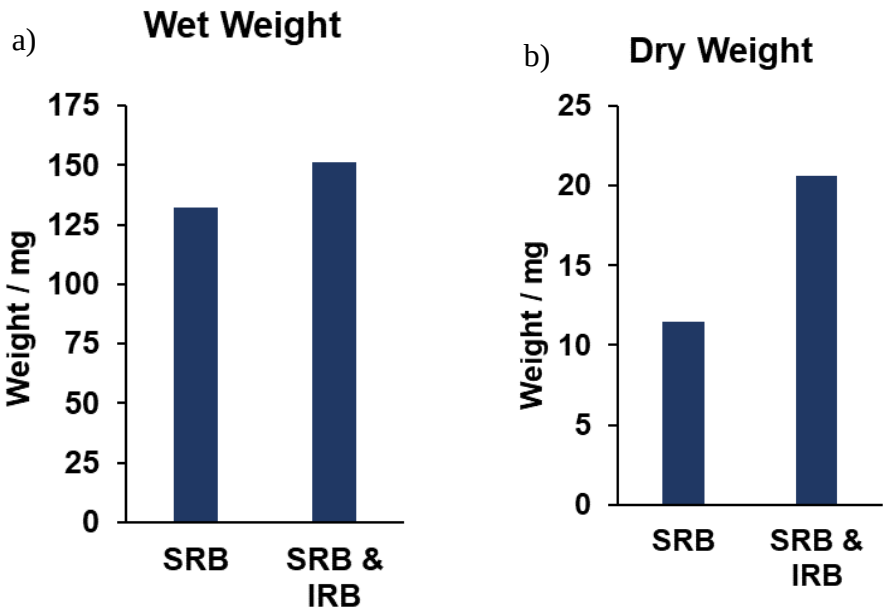


Figure 5-2. Quantity of bioagglomerates precipitated inside the closed bottled system SRB and SRB & IRB were added and incubated for 72 h. (a) represents the wet weight of the agglomerates

after centrifugation and (b) represents the dry weight of the agglomerates that are dried of moisture after centrifugation.

Figure 5-2 (a) showed the overall wet weight of the agglomerates after centrifugation for 10000 rpm for 10 minutes. It showed that the wet weight was higher in case of coculture when compared with the SRB pure culture systems. Even though there was difference between the weight of bioagglomerates, the difference was not so significant as the moisture present inside the centrifugate affected the value. In order to eliminate this, after centrifuging the tubes were dried inside hot air oven kept at 60°C for 12 hours and then taken for quantification. A significant difference in the bioagglomerates precipitated was observed after drying. It was observed that the dry weight of SRB and IRB coculture system was 44% higher than that of SRB pure culture system. This observation clearly establishes the impact of IRB on the overall bioagglomerates formation. Thus, the IRB can accelerate the SRB mediated FeS production and eventually increase the bioagglomerates formation.

5.2.3 Increased microbial growth in SRB and IRB coculture system

Since the bioagglomerate precipitation was shown to be accelerated inside the bottled system in the cocultures, the microbial community growth inside them can also be different in the coculture system when compared to that of pure culture systems. In order to check the microbial growth, the total protein concentration inside the system was observed at different time intervals (Figure 5-3). This analysis can be related to the bacterial growth and activity inside the bottled system.

The bacterial cell counts inside the coculture system were calculated at different time points along the course of FeS bio precipitation, the results as shown in the figure 5-4 showed that the total cell counts increased in both SRB pure culture and SRB and IRB coculture bottled systems with respect to time even after 72 hours of incubation. There was about 28% higher bacterial cell count observed in the SRB and IRB coculture system when comparing with the SRB pure culture bacterial systems.

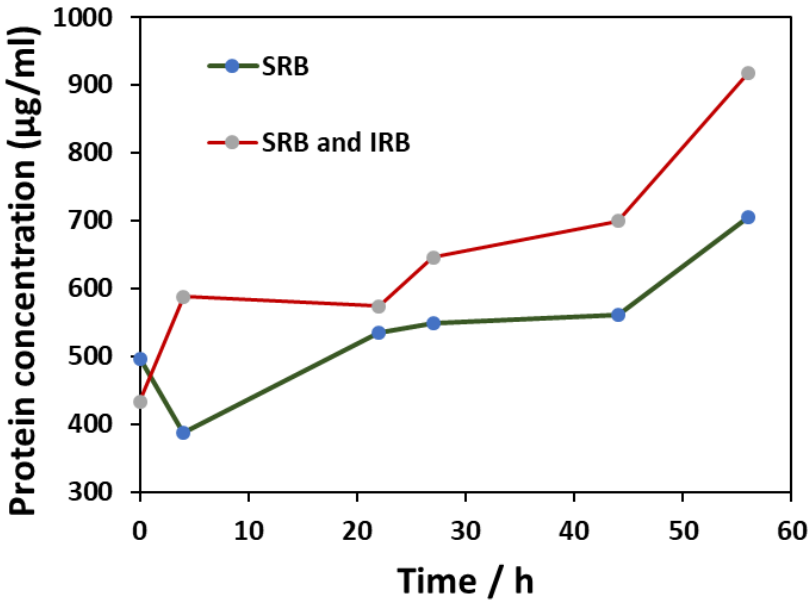


Figure 5-3 Total protein concentration measured inside the bottled cultures at different time intervals when SRB (green line) and SRB and IRB (red line) were added to the medium supplemented with 20mM lactate, 17 mM sulfate and 1.8 mM Fe^{2+}

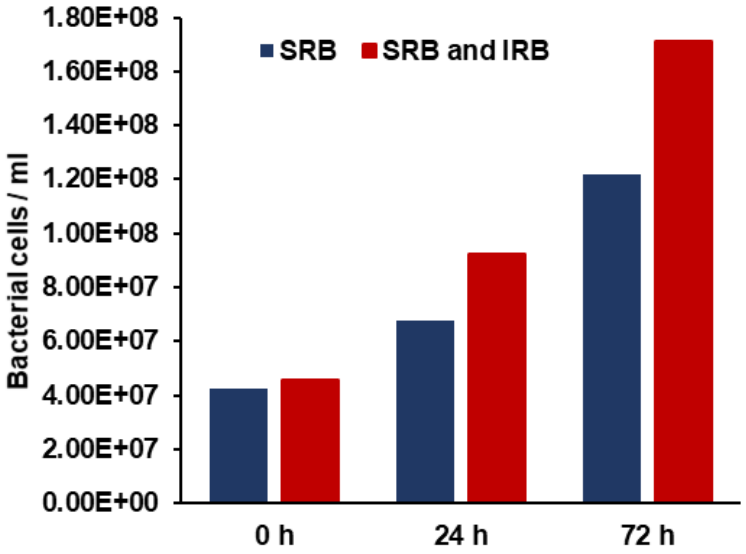


Figure 5-4 Total bacterial cell counts observed at different time intervals when SRB (blue) and SRB and IRB (red) were added to the bottled systems

5.2.4 Synergetic growth between SRB and IRB cells

The past observations have showed enhanced FeS generation and higher bacterial growth rate in the coculture system at bottled environments. Since the IRB are not capable of generating FeS, it can be considered that the SRB cells are growing inside the coculture systems, as the SRB pure cultures too showed growth without IRB inside the closed bottle system. It is evident that the IRB accelerated the SRB growth and activity but it is not sure whether SRB might have an influence on IRB growth. The distribution of IRB was studied by Fluorescent In situ Hybridization (FISH) ((Figure 5-5) which clearly showed that the IRB cells were increased in 72 hours cultivated coculture medium when compared to cell counts measured at 22 hours.

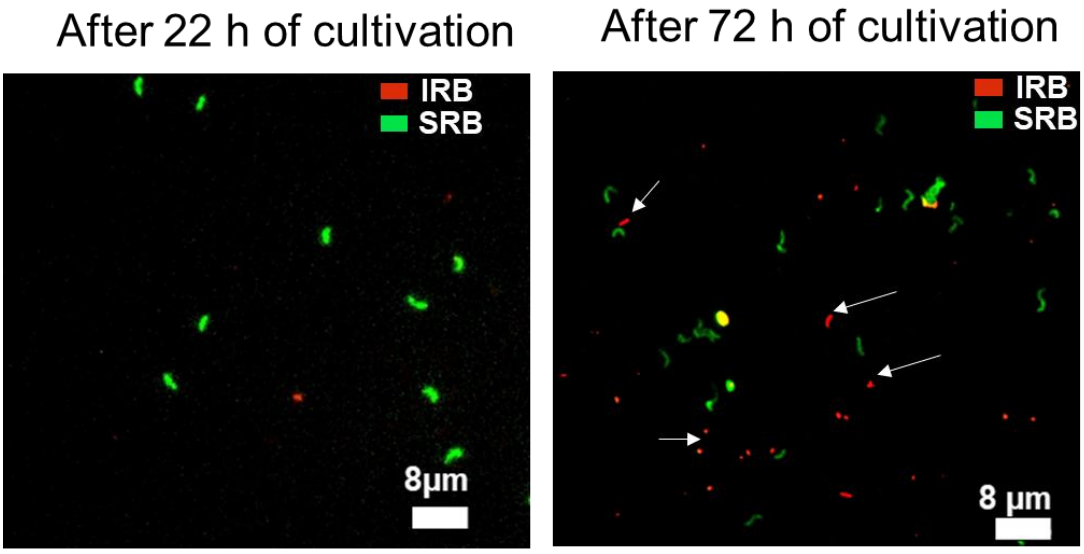


Figure 5-5 SRB and IRB distribution inside the SRB and IRB coculture bottled system as seen by Fluorescent in-situ hybridization (FISH) at different time intervals

This observation established that in the coculture system IRB growth was also supported, even without addition of any external electron acceptors. This opened up a new possibility that either SRB or the products released by SRB could act as a potential electron acceptor for the growth of IRB.

In order to check the synergetic interaction that accelerated the FeS generation and cell growth, certain mutant strains were used for the coculture experiments and the precipitation of FeS was observed. SRB shows formation of membrane bound FeS nanoparticles while they grow

which can be a potent factor involved in electron transferred across the membrane. The *ΔNiFeSe* mutant of SRB was checked in the coculture system for FeS bio precipitation (Figure 5-6 a). Usually this mutant showed lack of membrane bound FeS biomineralization in the SRB cells. However, the results showed no significant FeS precipitation when compared with SRB wildtype cocultures after 72 hours, thus eliminating the involvement of SRB membrane bound FeS on the accelerated FeS generation.

The outer membrane c-type cytochromes are involved in electron transfer across the cell membrane in IRB. They are crucial for electron transfer and we observed the effect of *ΔOmcAll* mutant on the overall FeS precipitation in the coculture system (Figure 5-6 b).

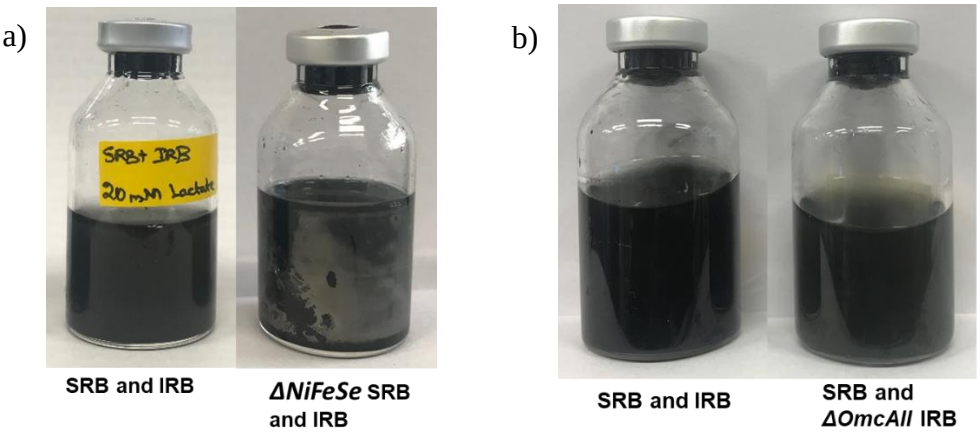


Figure 5-6 Precipitation of black FeS nanoparticles in the bottled system after having 20mM lactate, 17 mM sulfate and 1.8 mM Fe^{2+} compared with SRB and IRB wild type strains when (a) SRB and *ΔNiFeSe* SRB mutant and (b) SRB and *ΔOmcAll* IRB mutant were added.

With the *ΔOmcAll* IRB mutant delayed FeS precipitation was observed in the presence of SRB wild type strains. This hinted that the outer membrane cytochromes of the IRB might be involved in the synergetic interaction with the SRB cells. One explanation could be that deletion of the outer membrane C-type cytochromes limit the range of extracellular electron transfer with extracellular electron acceptors. This has potential to control the IRB growth and its activity which was reflected in the FeS generation in the cocultures.

5.2.5 Proposal for accelerated FeS generation by SRB in the presence of IRB

The enhanced FeS nanoparticles agglomeration inside the SRB and IRB coculture bottled system can be put alternatively explained as increase in sulphate reduction by the SRB. Higher generation of hydrogen sulphide reduced species will enhance its interaction with Fe^{2+} ions in the medium which settle as iron sulphide nanoparticles. Also, we observed growth of IRB cells inside this coculture system even without addition of external electron acceptors. This phenomenon can be explained by generation of electron acceptors by SRB. Moreover, reduced FeS precipitation while using IRB mutant lacking outer membrane cytochromes supports that electron transfer across these proteins might be crucial for the survival of IRB survival[119]. Since, the sulphate reduction was accelerated in the coculture system we propose that the metabolically generated electron from the IRB might be transferred to the SRB by the involvement of outer membrane cytochromes and can accelerate the sulphate reduction.

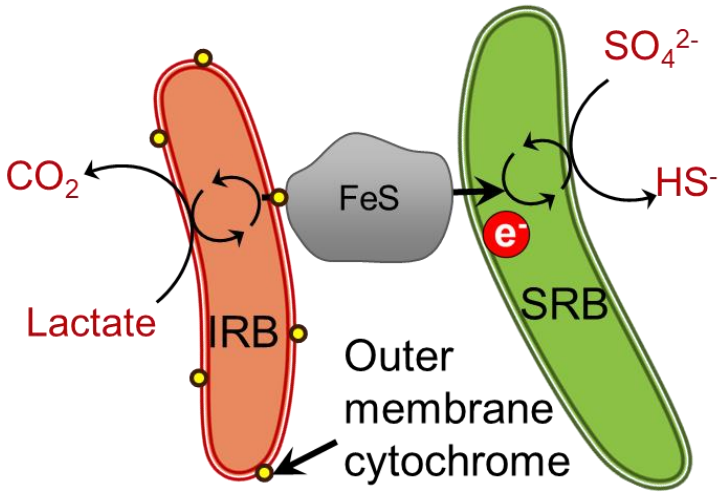


Figure 5-7 Proposed interspecies electron transport model between SRB and IRB.

5.3 Conclusion

The involvement of the iron reducing bacteria *S. oneidensis* MR-1 on acceleration of FeS nanoparticles agglomeration by the sulphate reducing bacteria *D. vulgaris* Hildenborough was studied. The coculture system also exhibited increased bacterial growth and activities when

compared to that of pure culture systems. The observation with IRB mutant lacking outer membrane cytochromes exhibited that extracellular electron transfer across the IRB membrane might be involved in the growth of IRB inside the coculture anoxic system. The possibility of IRB metabolically generated electron coupled sulphate reduction in the SRB can explain the accelerated FeS biosynthesis and synergetic growth inside the coculture system. With the current model of interspecies electron transfer mediated through conductive FeS, a positive feedback was observed between production of FeS by SRB and IRB growth. This explains possible synergetic growth associated with interspecies electron transfer occurring between SRB and IRB at natural environments.

References

1. He, Z.; Kan, J.; Mansfeld, F.; Angenent, L. T.; Nealson, K. H., Self-sustained phototrophic microbial fuel cells based on the synergistic cooperation between photosynthetic microorganisms and heterotrophic bacteria. *Environmental science & technology* **2009,** *43* (5), 1648-1654.
2. Deng, X.; Dohmae, N.; Kaksonen, A.; Okamoto, A., Biogenic Iron Sulfide Nanoparticles Enable Extracellular Electron Uptake in Sulfate‐Reducing Bacteria. Angewandte Chemie 2020.
3. Meitl, L. A.; Eggleston, C. M.; Colberg, P. J.; Khare, N.; Reardon, C. L.; Shi, L., Electrochemical interaction of Shewanella oneidensis MR-1 and its outer membrane cytochromes OmcA and MtrC with hematite electrodes. *Geochimica et Cosmochimica Acta* **2009,** *73* (18), 5292-5307.

Chapter 6

Microbial current generation enhancement by metal sulphide with better conductive properties

6.1 Introduction

The formation processes of metal sulfides in sediments, especially iron sulfides, have been the subjects of intense scientific research because of linkages to the global biogeochemical cycles of iron, sulfur, carbon, and oxygen.[1] However transition metal sulphide with considerably low solubility are also found to be formed in the sediments along with other minerals. Trace minerals of Ni, Cu, Zn, Mn, Mo, Co and Hg were found to be associate with iron sulphide minerals in the anoxic sediments. Mackinawite one of the widely observed FeS forms at sediments is incorporated with Ni trace metals which can considerably increase their conductivity.[1-5]

Although iron mono sulphides in their mackinawite form shows excellent metallic like electrical conductivity properties, there are many other transition metal sulphides which can have better electrical properties than the FeS.[6] Other than improving better electrodes with good electrical properties, one of the limitations of SMFC is to have a better conductive sedimental substrates.[38-39] Since the anoxic sub surfaces can be composed to have these transition state metal sulphides, they can be used to improve the SMFC performances.[1] Earlier reports showed that even with some semiconductors the extracellular electron transfer for electroactive microbes can be increased.[7-8] The metal sulphides for improving the microbial electricity generation.

The metal sulphides are precipitated by microbially released hydrogen sulphides when on reaction with the metal ions form metal sulphides. The solubility of formed metal sulphides are found to be considerably low which means the precipitation of the metal sulphides will occur.[9-10] Earlier reports showed detection of many metal ions in the sedimental pore waters. Thus, this form a perfect environment for sedimentation on metal sulphides in the anoxic sediments.[130] [131]In this work we studied the impact of different metal sulphides formation on the overall electricity generation from the microbes.

6.2 Results and Discussion

6.2.1 Microbial electricity generation with different metal ions

The effect of metal ions on anodic current generation in the SRB and IRB cocultures was studied. The activity of SRB produces hydrogen sulphides which are readily reacted with the metal ions and precipitate metal sulphides. Also, there is a risk of toxicity from these metal ions on the bacterial growth. In order to check this, very low concentrations of 100 µM of different metal ions such as nickel, copper and molybdate (MoO_4^{2-}) were added to different coculture electrochemical systems consisting 20 mM lactate, 17 mM sulphate (Figure 6-1). The anodic potential was setup at +0.2 V vs Ag/AgCl reference electrode and the current produced inside the system was observed. Figure 6.1 shows the current obtained when different metal ions were added to the electro chemical system.

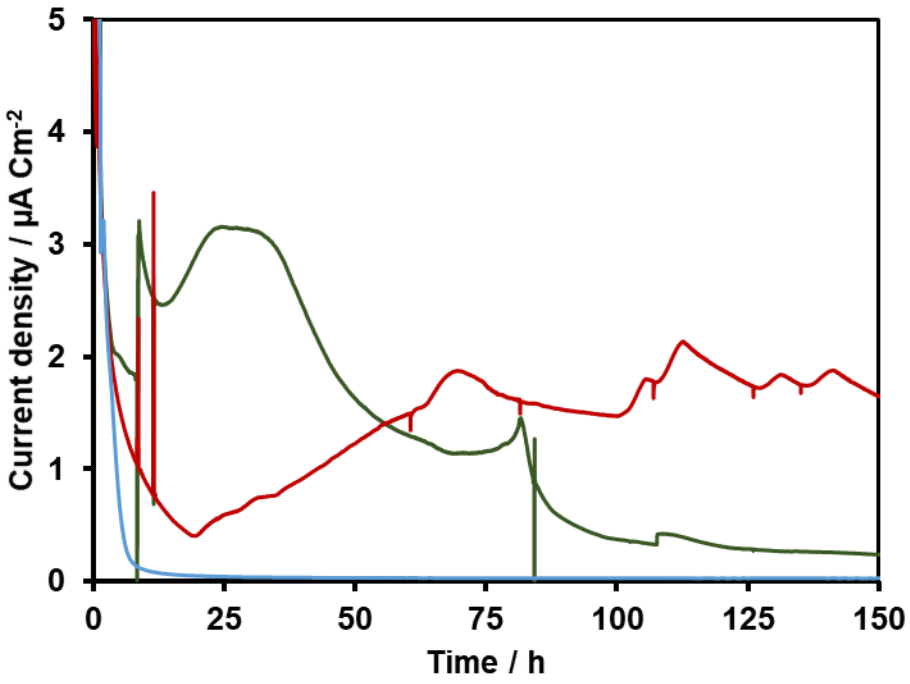


Figure 6-1 Anodic current generation in the SRB and IRB coculture system supplemented with 20 mM lactate, 17 mM sulphate, 100 µM Cu^{2+} (blue line), 100 µM Ni^{2+} (red line), 100 µM molybdate (green line)

Cocultures with Ni^{2+} and Molybdate showed microbial current generation whereas there was no current generation observed when Cu^{2+} was added. This can be partially explained that Cu2+ is a potent toxic substance for microbial growth, whereas the microbes are able to survive with 100 µM of Ni^{2+} and Molybdate. The Molybdate added medium showed maximum peak current density around 3.1 µA/cm^2 observed around 24 hours and then it reduced until 75 hours where a small current increase peak was observed soon followed by steep decrease in the current. This current was not recovered even after addition of 20mM lactate after current depletion. One explanation could be that most of the cells would have died inside system and that was reflected in no current increase even after lactate addition. In the presence of Ni^{2+} there was a gradual increase in current generation observed after 23 hours which was maintained even until 125 hours.

6.2.2 Microbial electricity generation with different metal ions in the presence of FeS bioprecipitates

Since the heavy metals added to the electrochemical can be toxic at lower cell counts, their toxicity can be overcome when they are added at higher SRB and IRB cell counts. Hence, we observed the effect of metals addition on the coculture current generation having Fe^{2+} during FeS bio agglomeration (in Figure 6-2). The combination of iron sulphides with other metal sulphides could be impacting the bioagglomerates conductivity. So, initially the 1.8 mM of Fe^{2+} was added to the electrochemical system supplemented with 20 mM lactate, 17 mM sulphate and poising the working electrodes at + 0.2 V. After initial few hours, the precipitation FeS started to happen accompanied by increase in the anodic current production. Right now, the SRB and IRB cell counts are higher enough to withstand the metal ions toxicity. Thus 100 µM of Ni^{2+}, Cu^{2+} and molybdate were added individually in different systems.

The slope of anodic current generation was increased significantly when Ni^{2+} was added to the electrochemical reactor around 118 h directly indicating the positive the impact of nickel sulphide mineralization inside the electrochemical reactor. The molybdate was added to the reactor where 20mM lactate was added after lactate depletion around 127 hours. Initially there was a lag period where the current generation was reduced until 142 hours after which the current production recovered which kept on increasing with a peak current of 10.5 µA/cm^2 observed after 191 hours. This peak current was higher than that observed only with FeS formation. Usually whenever lactate was added after the lactate depletion the second peak current always showed similar values to that

of the initial current obtained. However, here the presence of molybdate had increased the current generation. In the case of Cu^{2+} addition during active FeS precipitation, a sudden depletion in the anodic current was observed which gradually recovered over time. There was not a significant positive change in current slopes values were obtained indicating that Cu^{2+} might be still affecting the microbial activities despite forming highly conductive copper sulphides. Additionally, the impact of Mn^{2+} on the current generation was also observed to the system having Fe^{2+} and Ni^{2+}. After the slope increase by Ni^{2+} addition in the FeS bio agglomeration system, further 100 µM of Mn^{2+} was added. Interestingly, even this time the slope of current was increased further upon Mn^{2+} addition. Thus, from this it was evident that the formation of manganese sulphide positively impacted the current generation.

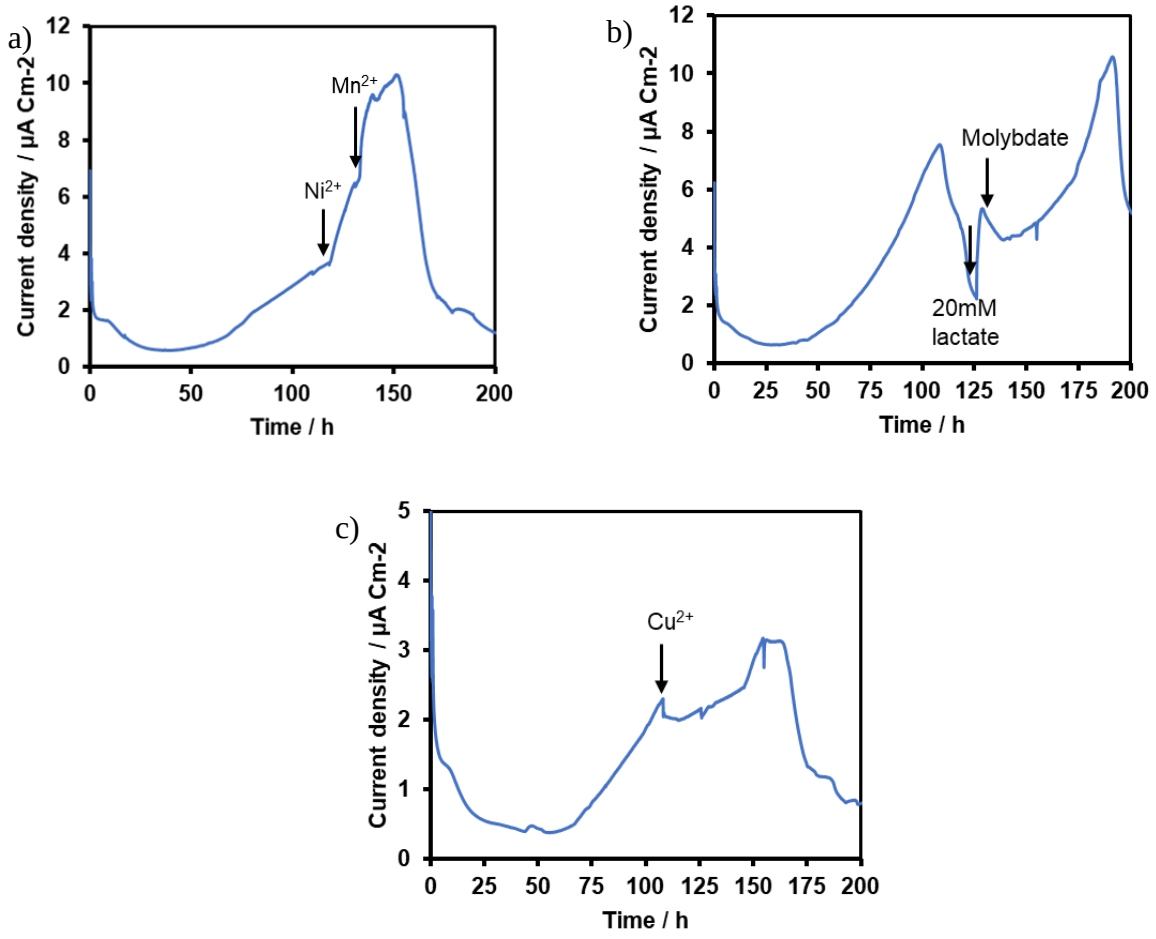


Figure 6-2 Representative anodic current generation in electrochemical SRB and IRB coculture system supplemented with 20 mM lactate, 17 mM sulphate, 1.8 mM Fe^{2+} where Ni^{2+} and Mn^{2+} (a),

Molybdate (b) and Cu^{2+} (c) were added. The arrow marks indicate the time point at which the substrates were added.

6.3 Conclusion

The effect of various metal ions on microbial current generation was obtained. Even though, the bacterial current generation was increased with formation of other metal sulphides, presence of Cu^{2+} inhibited the current generation indicating its toxicity. The toxicity level was controlled in a system having active FeS generation indicating that combination of different metal sulphides can help to overcome heavy metal toxicity effect on the microbial current generation. Combination of other metal sulphides with the FeS biomineralization also showed a positive response in the overall current generation. Even the formation of manganese sulphides which exhibit relatively semiconducting property also increase the microbial current generation. These finding has open immense opportunities of using a wide range of metal sulphide precipitates which can be used to improve the electron transfer rates across the anoxic sediments. Possibility of long-range electron transfers improved with highly conducting metal sulphides would efficiently increase the current generation from sediments.

References

1. Wilkin, R. T., Sulfide minerals in sediments. In Encyclopedia of Sediments and Sedimentary Rocks, Middleton, G. V.; Church, M. J.; Coniglio, M.; Hardie, L. A.; Longstaffe, F. J., Eds. Springer Netherlands: Dordrecht, 2003; pp 701-703.
2. Luther, G. W.; Meyerson, A. L.; Krajewski, J. J.; Hires, R., Metal sulfides in estuarine sediments. Journal of Sedimentary Research 1980, 50 (4), 1117-1120.
3. Raiswell, R.; Plant, J., The incorporation of trace elements into pyrite during diagenesis of black shales, Yorkshire, England. Economic Geology 1980, 75 (5), 684-699.
4. Huerta-Diaz, M. A.; Morse, J. W., Pyritization of trace metals in anoxic marine sediments. Geochimica et Cosmochimica Acta 1992, 56 (7), 2681-2702.
5. Li, Y.; Kitadai, N.; Nakamura, R., Chemical diversity of metal sulfide minerals and its implications for the origin of life. Life 2018, 8 (4), 46.
6. Pearce, C. I., Electrical and Magnetic Properties of Sulfides. Reviews in Mineralogy and Geochemistry 2006, 61 (1), 127-180.
7. Lenin Babu, M.; Venkata Mohan, S., Influence of graphite flake addition to sediment on electrogenesis in a sediment-type fuel cell. Bioresource Technology 2012, 110, 206-213.
8. Zhou, Y.-L.; Yang, Y.; Chen, M.; Zhao, Z.-W.; Jiang, H.-L., To improve the performance of sediment microbial fuel cell through amending colloidal iron oxyhydroxide into freshwater sediments. Bioresource Technology 2014, 159, 232-239.
9. Jiang, X.; Hu, J.; Lieber, A. M.; Jackan, C. S.; Biffinger, J. C.; Fitzgerald, L. A.; Ringeisen, B. R.; Lieber, C. M., Nanoparticle Facilitated Extracellular Electron Transfer in Microbial Fuel Cells. Nano Letters 2014, 14 (11), 6737-6742.
10. Qian, F.; Wang, H.; Ling, Y.; Wang, G.; Thelen, M. P.; Li, Y., Photoenhanced electrochemical interaction between Shewanella and a hematite nanowire photoanode. Nano letters 2014, 14 (6), 3688-3693.
11. Bryson, A.; Bijsterveld, C., Kinetics of the precipitation of manganese and cobalt sulphides in the purification of a manganese sulphate electrolyte. Hydrometallurgy 1991, 27 (1), 75-84.
12. Gharabaghi, M.; Irannajad, M.; Azadmehr, A. R., Selective sulphide precipitation of heavy metals from acidic polymetallic aqueous solution by thioacetamide. Industrial & Engineering Chemistry Research 2012, 51 (2), 954-963.

13. Jandova, J.; Lisa, K.; Vu, H.; Vranka, F., Separation of copper and cobalt–nickel sulphide concentrates during processing of manganese deep ocean nodules. Hydrometallurgy 2005, 77 (1-2), 75-79.
14. Webb, J.; McGinness, S.; Lappin-Scott, H., Metal removal by sulphate-reducing bacteria from natural and constructed wetlands. Journal of Applied Microbiology 1998, 84 (2), 240-248.

Chapter 7

General conclusion and future prospects

7.1 General Conclusion

In the present thesis, the impact of biomineralized iron sulphides by the sulphate reducing bacterium *Desulfovibrio vulgaris* Hildenborough on the synergetic current generation with the iron reducing bacterium *Shewanella oneidensis* MR-1. Their interaction with each other and with the FeS bioprecipitates on the anodic current generation was studied.

Initially, in Chapter 3, the interaction of the SRB pure culture *D. vulgaris* Hildenborough with the anode was observed. The presence of FeS bioagglomerate impacted the overall current generation. Many of the earlier reports showed the hydrogen sulphide mediated abiotic oxidization coupled electron transfer at the anodes. However, we observed that in addition to the above-mentioned mechanism, FeS precipitation also dominated the current generation. The anodic current generation was declined after the lactate depletion stage which was characterized by oxidative loss of FeS on the anodes. The iron sulphides were found to be attached to the SRB membrane. A new proposal for FeS mediated electron transfer to the anodes from the SRB was proposed in this study. Understanding of new pathways would help to improve the design and operation of SRB MFCs.

In Chapter 4, the symbiotic current generation in the SRB and IRB were studied along with the importance of bioagglomerates of FeS. The anodic current generation in the SRB and IRB coculture electrochemical system was many folds higher than that of the current produced by IRB pure cultures. In these synergetic current production mechanisms, the impact of conductive iron monosulphides formation was seemed to be evident. SEM observations showed formation of FeS bioagglomerates with the bacterial cells embedded in them. Much thicker bioagglomerates were observed in the coculture systems when compared with the SRB and IRB pure cultures separately. This opened up the importance of long-range electron transfer across the bioagglomerates which increased the electron transfer to the anodes. Performance of source-drain electrochemical experiments showed the importance of FeS based long-range electron conduction in the

bioagglomerates. These observations showed that the presence of much higher conductive bioagglomerates can increase the power output of sediment microbial fuel cells.

Chapter 5 showed the symbiotic interactions between SRB and IRB on FeS bio precipitation and increased bacterial growth. The findings showed that the presence of IRB accelerated the FeS precipitation by the SRB which was higher when compared to that of SRB pure cultures. Similarly, the increase in total bacterial cell counts was higher in the SRB and IRB coculture systems which also showed increase in the total protein contents much higher than that of SRB pure cultures. With observations from the IRB mutant strain lacking outer membrane cytochromes, an interspecies electron transport model was proposed for the synergetic interactions where the metabolically generated electrons of IRB are coupled to sulphate reduction by SRBs.

Chapter 6 explained the improvement of microbial current generation by the precipitation of metal sulphides with better electrical properties. Addition of Ni^{2+} and molybdate both showed current generation although each showed different current generation profiles. The toxicity of Cu^{2+} to the bacterial cells prevented electricity generation which can be reduced in a system having more bacterial cell counts and active FeS bio precipitation.

In this thesis, it has been proved that the microbial current generation at the anodes can be increased by forming bioagglomerates having efficient conductive iron sulphides. The microbial interactions that happen at the anode surfaces can influence the iron sulphide precipitation and thereby impact the anodic current generation. This phenomenon can be applied in SMFCs to improve their performances. Even though FeS is the most abundant mineral observed at the anoxic sediments, inclusion of other metal sulphides to the sediments can increase the electricity production.

7.2 Future prospects

From the current study, it was emphasized that the microbial current generation can be enhanced in the presence of conductive bioprecipitates. With lower power densities, the cost of production for the SMFCs are higher as there is a need for larger surface area for the electrodes. However, by using systems having conductive bioprecipitates the current densities at the electrodes can be increased many folds. This can potentially reduce the surface area of the electrodes being used for the SMFC devices. Thus, the cost for establishing the SMFC units can be reduced. The findings of this work can be employed in developing subsurface electrical grids.

New ideas are being proposed to develop underwater electrical interconnections to power various devices that require high electrical power. Thus, increasing the SMFC performances are always going to improve the development of subsurface electric grids.

The microbial interactions between the sulphate reducing bacteria and the iron reducing bacteria has been observed to be syntrophic increasing the microbial activities and subsequently the sulphate reduction to precipitate iron sulphides. According to the present ideas the dominant bacteria can outgrow at competing environments. However, our current observations showed that the symbiotic interactions between bacteria can actually benefit growth of different microbial communities. The electron transfer between SRB and IRB can favor efficient energy utilization in energy limiting environments.

The symbiotic interactions between IRB and SRB enhanced the sulphate reduction by SRB significantly. Provided that the microbial based sulphate reduction is impacting the global bio-geochemical sulphur cycles, the synergetic interactions of the Sulphate reducing bacteria with the other microbes will have a considerable shift in the sulphur cycles globally.